ISOLATED NUCLEUS STIFFENS IN RESPONSE TO LOW INTENSITY VIBRATION

by

Joshua Newberg

A thesis

submitted in partial fulfillment

of the requirements for the degree of

Master of Science in Mechanical Engineering

Boise State University

December 2019

© 2019

Joshua Newberg

ALL RIGHTS RESERVED

BOISE STATE UNIVERSITY GRADUATE COLLEGE

DEFENSE COMMITTEE AND FINAL READING APPROVALS

of the thesis submitted by

Joshua Newberg

Thesis Title: Isolated Nucleus Stiffens in Response to Low Intensity Vibration

Date of Final Oral Examination: 20 November 2019

The following individuals read and discussed the thesis submitted by student Joshua Newberg, and they evaluated the student's presentation and response to questions during the final oral examination. They found that the student passed the final oral examination.

Gunes Uzer, Ph.D.	Chair, Supervisory Committee
Clare Fitzpatrick, Ph.D.	Member, Supervisory Committee
Paul Davis, Ph.D.	Member, Supervisory Committee
Trevor Lujan, Ph.D.	Member, Supervisory Committee

The final reading approval of the thesis was granted by Gunes Uzer, Ph.D., Chair of the Supervisory Committee. The thesis was approved by the Graduate College.

DEDICATION

I dedicate this to my creator and lord as a stepping-stone to further my career in mental, physical, and spiritual health optimization.

ACKNOWLEDGMENTS

I would like to acknowledge my mother because I would not be in this position without her drive, commitment, and love for her sons. I would also like to acknowledge all former wrestling coaches, teammates, and supporters. Without the characteristics learned from that sport I would not be the driven person that I am. I would also like to acknowledge Dr. Uzer for giving me the opportunity to be a graduate student in the MAL.

ABSTRACT

The nucleus, central to all cellular activity, relies on both direct mechanical input and its molecular transducers to sense and respond to external mechanical stimuli. This response occurs by regulating intra-nuclear organization that ultimately determines gene expression to control cell function and fate. It has long been known that signals propagate from an extracellular environment to the cytoskeleton and into nucleus (outside-in signaling) to regulate cell behavior. Emerging evidence, however, shows that both the cytoskeleton and the nucleus have inherent abilities to sense and adapt to mechanical force, independent of each other. While it has been shown that isolated nuclei can adapt to force directly *ex vivo,* the role of nuclear mechanoadaptation in response to physiologic forces *in vivo* remains unclear.

To gain more knowledge regarding nuclear mechanoadaptation in cells, we have developed an atomic force microscopy based experimental procedure to isolate live nuclei and specifically test whether nuclear stiffness increases in mesenchymal stem cells (MSCs) following the application of low intensity vibration (LIV). Results indicated that isolated nuclei were on average 36% softer than nuclei of intact MSCs. In intact MSCs, depletion of nuclear structural proteins LaminA/C and Sun-1&2 led to both decreases in nuclear elastic moduli and decreased chromatin condensation in Sun-1%2 depleted samples. In isolated nuclei, identical depletions led to decreased stiffness and significantly higher chromatin decondensation levels (47% & 39% increase for LaminA/C and Sun-1&2 nuclei respectively). When LIV was applied in series (0.7g,

90Hz, 20min) either twice (2x) or four times (4x), increased nuclear stiffness of intact MSCs showed dose dependency while stiffness changes in isolated nuclei was only detectable at the 4x LIV dose. Changes in isolated nuclear stiffness was not accompanied by changes in Lamin A/C or Sun1&2 protein levels. Interestingly, chromatin measurements in isolated nuclei showed a 25.4% smaller chromatin to nuclear area size in 4x LIV nuclei compared to controls.

TABLE OF CONTENTS

LIST OF FIGURES

LIST OF EQUATIONS

LIST OF ABBREVIATIONS

ECM	Extracellular Matrix
MSC	Mesenchymal Stem Cell
FAK	Focal Adhesion Kinase
FA	Focal Adhesion
LIV	Low Intensity Vibration
LINC	Linker of nucleoskeleton and cytoskeleton
AFM	Atomic Force Microscopy

CHAPTER ONE: INTRODUCTION

1.1 Research Motivation

The human body consists of approximately 30 trillion cells, which all serve specific functions. Among these cells are stem cells. Stem cells are progenitor cells, that go through a differentiation process to create all human cell types. [1] Stem cells are generalized cells that differentiate into specialized lineages. There are four main types of stem cells: hematopoietic, responsible for blood cell differentiation, neural, responsible for the neurocytes, brain tissue and nervous system, epithelial cells, responsible for cells that make up skin and organ tissue, and mesenchymal stem cells, responsible for bone, [8] cartilage, fat, and muscle tissue. Stem cells are critical players in body function and maintenance given the fact that they self-renew to create bodily tissues and regenerate damaged tissue. These processes of self-renewal and regenerations are known as proliferation and differentiation. Surprisingly, stem cells only make up 1-2% of the tissue cell population. [1] Among these stem cell types, mesenchymal stem cells (MSCs) make up the musculoskeletal tissues that serve in human locomotion (bone, cartilage, fat, and muscle[1]). In bone, MSCs reside within close proximity (100-300μm) of bone surfaces within bone marrow[1]. During daily activities like walking or running, MSCs experience inertial, tensile, compressive, and fluid flow induced shear forces[2]. It is understood that MSCs are mechanically adaptive, meaning that they sense and respond to mechanical forces present in their environment. MSC locomotion, contractility, and force sensing is largely facilitated by a network of cytoskeletal components, which transmit forces

directly to the control center of the cell; the nucleus.[14] The nucleus, in turn, controls cell function and fate by regulating the gene expression.[10] In this way, gene expression and overall cell function are in-part dependent on the magnitude, frequency and duration[2] of external forces. Though the cell, as a whole, has long been recognized as a mechanoadaptive structure, it has only recently been uncovered that the nucleus, a mechanoresponsive element, plays a large role in the mechanotransduction (force transfer) process.[11]

The nucleus has been shown to have a structural system of its own known as the nucleoskeleton. The nucleoskeleton is integrated with cytoskeletal components and is involved in nuclear motility and organization of chromatin (DNA).[14] Chromatin regulation and gene transcription control cell function. In this way, changes in nuclear structure and mechanics are emerging as important regulators of cell function. [21] Changes in nuclear structure in the form of stiffening, nuclear membrane reorganization, and chromatin organization are involved in MSC differentiation into tissue-specific cell types.[51] On the flip side, drivers of debilitating diseases such as muscular dystrophy, progeria, cardiomyopathy, cancer, and premature aging are evident in irregular nuclear membrane structure and chromatin organization.[50] Despite this growing knowledge of how cells interact with their external environment through cytoskeletal interactions, a critical knowledge gap exists in understanding how nuclei adapt to specific external forces, *in vivo.*

Our motivation of this work is to address this knowledge gap by developing a robust method to study how nuclear mechanics, independent of the cell, adapt to changes in cytoskeletal contractility in response to extracellular force. This method will

ultimately allow us to study how changes in the cytoskeletal contractility, in response to extracellular forces, affects nuclear mechanics, function and overall cell fate.

1.2 Specific Experimental Goal and Hypothesis

The specific goal of this research is to quantify the nuclear response to low intensity vibration by measuring changes in nuclear stiffness, morphology, structural changes of the nucleoskeleton and chromatin organization. We hypothesize that the nucleus will respond to low intensity vibration by way of stiffening. Identifying how the entire nuclear structure adapts to specific mechanical forces, applied at the cell level, will allow us to study force-regulated pathways in the nucleus. This research can help bridge the knowledge gap in the development of specific force application techniques, which guide differentiation of MSCs and contribute to tissue regeneration in bone and cartilage. In addition, successful research will provide insight in how disease-related changes in tissue mechanics result in altered nuclear mechanics and function.

CHAPTER TWO: BACKGROUND

2.1 Mesenchymal Stem Cell

Stem cells are responsible for the creation of all cells in the human body. That is, stem cells proliferate and differentiate into all cells that make-up the entirety of human body tissue. During development, embryonic stem cells can form any type of cell in humans by committing to specialized stem cell types[1]. These tissue specific stem cells can divide and renew themselves for relatively long periods of time. Stem cells serve as a tissue generation and repair system by replenishing cells throughout a person's lifetime. In bone, the resident stem cell type is a Mesenchymal Stem Cell (MSC). MSCs are a specific type of multipotent stem cell which can differentiate into bone (osteoblast), muscle (myocyte), cartilage (chondrocyte), and fat (adipocyte)[46]. MSCs reside mainly in bone marrow, near the bone surface, and take on a large responsibility in the creation and maintenance of bone tissue through their differentiation into osteoblasts, which lay down new bone tissue, and further into osteocytes, which sense forces throughout the tissue. MSCs are also responsible for maintaining articular cartilage tissue due to their ability to differentiate into chondrocytes during initial growth phases or from cartilage trauma. [52] MSCs rely on, and are rather controlled by, mechanical stimulation, present in their environment, for ultimate decision making. Independent studies have confirmed this idea through applied tension, compression, fluid shear, and accelerations on MSCs. Results indicate that forces dictate cell fate through changes in gene transcription[15] and less understood mechanotransduction process within the cell nucleus. Understanding the

specific mechanisms which regulate stem cell differentiation, through mechanotransduction processes, will help researchers understand the driving force behind tissue-specific differentiation.

2.2 Cellular Mechanical Environment

Resident cells in locomotive tissues (MSCs, osteoblasts, chondrocytes, myocytes and adipocytes) are subject to multiple types of mechanical stimuli including, strain, fluid shear, compression, and acceleration forces, due to their environmental factors. One example occurs in bone tissue. In its natural environment, bone is under a constant state of remodeling. Daily activities and exercise create cyclic compression and tensile loading on bones. This loading creates fluid flow within the bone lacunar-canalicular networks[48] that is further translated into biophysical cues within osteocytes, in turn promoting bone anabolsim[2]. Additionally, independent experiments have shown that forces in the form of low magnitude, high frequency micro-strains increase bone formation rates. [25] Contrary to bone remodeling, disuse or prolonged unloading leads to significant bone loss. [25] Bone a major example of how mechanical stimulation regulates tissue structure.

Another example of a mechanically regulated tissue occurs in human joints. Articular cartilage (AC) exists on the epiphysial surface of adjacent bones. In initial bone and cartilage development MSCs differentiate into chondrocytes that are in part responsible of AC development. AC is a stress bearing tissue that distributes loads between bones that make up the joint. During physiological loading (walking, running, jumping), AC experiences hydrostatic pressure, synovial fluid shear, and strain that all vary throughout the cartilage depth. [53] Loading influences chondrocyte activity and decisions.[53] In fact, independent studies on chondrocytes *in vitro* show compressive

loading on MSCs influences chondrogenic differentiation by upregulating TGFB-1[54] (transforming growth factor). It is evident that cells, particularly MSCs, responsible for tissue growth and repair, are regulated by mechanical stimulation. But how does this mechanotransduction process work inside of the cell, thus, influencing its decisions?

2.3 Cytoskeleton Mechanotransduction

On a cellular level, MSCs respond to external force by generating their own internal forces to maintain homeostasis.[30] It has been studied that forces, applied to the exterior of the cell via extracellular matrix (ECM), propagate through the cell, via cytoskeletal components, and reach the nucleus, ultimately influencing organization and function of the cell. Mechanical forces first sensed at the exterior surface of the cell are turned directly into biochemical signals through the actin cytoskeleton, which result in changes in composition, organization, and function of the MSC. Starting in the ECM and working towards the interior, focal adhesions (FAs), are responsible for first contact of mechanical forces and reside in the ECM. The FA is a multiprotein structure composed of multiple layers (integrin signaling, force transduction, and actin regulatory layers) with each layer consisting of two to three different types of proteins. FAs are both direct lines of communication and attachments between the ECM and actin stress fibers[4]. Forces transferred from FAs directly influence density and organization of actin filaments through the regulation of actin polymerization[5]. Actin filaments are composed of G-actin subunits. Actin filaments go through constant restructuring: polymerization or depolymerization that is regulated from actin binding proteins. Actin filaments are heavily responsible for cell motility and are essential components of force transfer throughout the cell.

2.3.1 Mechanical Loads Influence Cytoskeletal remodeling

Mechanical signals sensed at the ECM trigger phosphorylation of Focal Adhesion Kinase (FAK) – a known activator of focal adhesion signaling, which recruits mTORC2, AKT and then Ras Homology Protein (RhoA). RhoA pathway is responsible for cell motility through activating actomyosin contractility. Contraction of actomyosin, actin fibers, creates cell motion. Mechanical forces, in the form of axial strain, also prove to increase RhoA phosphorylation[23], thus activating the myosin chain and actin filaments. In this study, high magnitude strains (2%, 0.17Hz) were applied to cells on a pliable substrate. This process shows one example of how forces applied to the extracellular matrix play a critical role in cell motility. Several methods currently exist to measure and quantify the role of the cytoskeleton in mechanotransduction: the cell's ability to translate and respond to internal and external forces. One study applied oscillatory fluid shear at a low physiological range (1Hz, +/- 0.4Pa) to MSCs over a period of one-hour. [55] Results indicated that the filamentous actin fibers started to align parallel to fluid shear direction after thirty minutes of shear, becoming almost completely parallel one-hour into shear. Overall, oscillatory shear stress showed direction reorganization of F-actin through β-catenin/Wnt signaling pathway that is known to regulate differentiation of MSCs to osteocytes or adipocytes. Other existing methods have utilized magnetic tweezers to stretch individual cells, [56] compression of MSCs in scaffolds, shown to influence chondrogenic differentiation through upregulated TGF- β pathway [54] Atomic Force Microscopy as a means of individual cell and nuclear compression,[56] and several others.

Mechanical stimulation on MSCs is of high interest in the scientific community, due in part to the reorganization of the cytoskeleton and further influences on cellular fate

and function. In agreeance, improper mechanotransduction function involving disruptions of the actin cytoskeleton, is associated with diseases including skeletal disorders and muscular dystrophy. [5] Conversely, disrupting cytoskeletal elements, RhoA, by inhibiting mTORC1 and mTORC2, disable metastasis activity in cancer cells.[49] It is understood that mechanical signals influence cytoskeletal dynamics. We must further investigate current literature to understand how these mechanical cues are influencing the control center of the cell: the nucleus.

2.4 Mechanotransduction Components of the Nucleus: Sun-1&2, LaminA/C, and Chromatin

Further downstream in the mechanotransduction process comes a point where the Actin cytoskeleton binds with the nucleoskeleton. The nucleus is the largest and stiffest organelle in the MSC. It contains all genetic information in the cell and through regulation of these genes, determines cell function. Forces transferred from the cytoskeleton to the nucleus, is now understood to influence gene regulation. Determining the mechanotransduction forces to the nucleus, actin fibers of the cytoskeleton connect directly to Nesprin proteins, that then bind to Sun-1 and Sun-2 protein structures. This organization of components that involves the coupling between both cytoskeleton and nucleoskeleton is known as the nuclear LINC complex (Linker of Nucleoskeleton and Cytoskeleton)[50] (Figure 1). The nuclear LINC complex consists of all members within and adjacent to the outer nuclear and inner nuclear membranes. The LINC complex serves in the direct transfer of force from the exterior of the cell to the intranuclear components. Sun-1&2 proteins exist between the outer and inner nuclear membrane. These are intermediary members which connect the actin cytoskeleton, through Nesprin

to a main structural member of the nucleus known as nuclear lamins, specifically LaminA/C. Current research has shown that Sun-1&2 and nuclear lamins play key roles in structural integrity and mechanical regulation of the MSC nucleus. One group applied mechanical stretching to nuclei *ex vivo* directly to Nesprins and observed a stiffening response over increased number of stretches[11]. They showed that depleting both Sun-1&2 and LaminA/C elements, individually from the nuclear membrane, completely inhibited nuclear response to tension. LaminA/C are type V intermediate filament proteins that

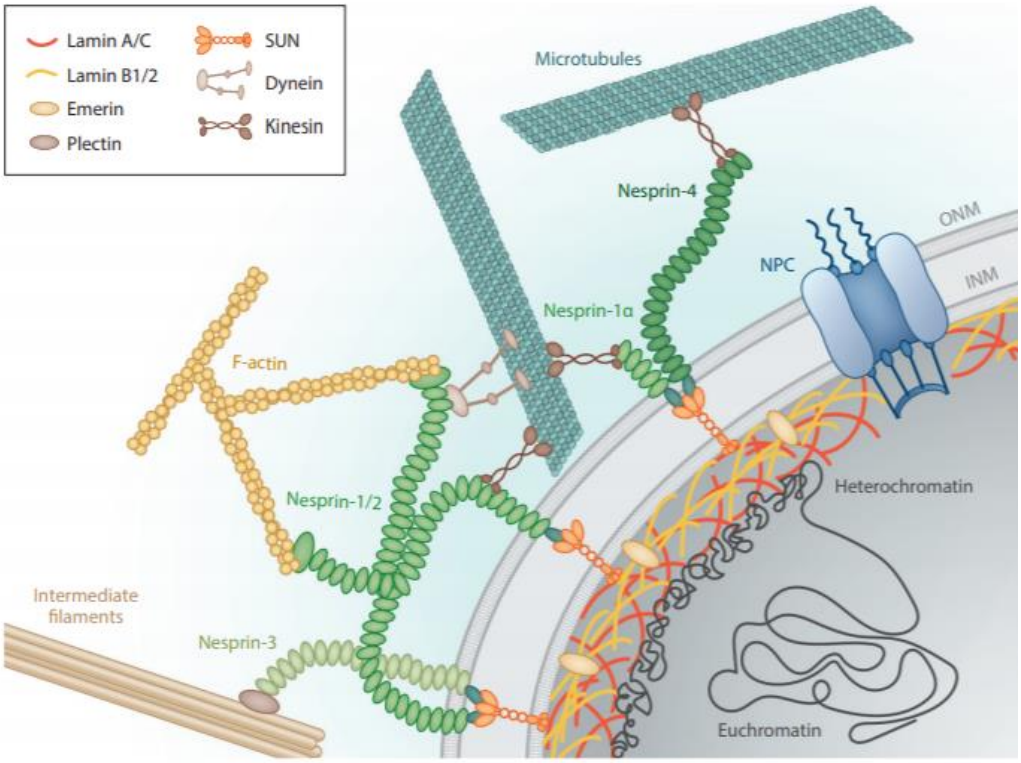

Figure 1. Nuclear LINC complex[14]

exist as a network adjacent to the intranuclear membrane. LaminA/C play a critical role in structural regulation of the nucleus including shape, stability, and stiffness.[7, 45] LaminA/C then directly binds to outer chromatin regions known as heterochromatin, further transferring forces sensed from the ECM deep into the nucleus. Currently, force

transfer from Nesprin to nuclear Sun 1&2 and lamins, and deeper into chromatin regions, dictate cellular mechanoresponse.

The nucleus is a mechanoresponsive organelle integrated with cell structure through its direct tie with cytoskeleton dynamics through the nuclear LINC complex.[14,15] When forces applied directly to the nucleus *ex vivo*, resulting in strain deformations, nuclei respond by stiffening through tyrosine phosphorylation of emerin[11], suggesting that the nucleus is an active contributor to mechanotransduction. Changes in the nuclear structure in turn influences gene transcription and cell differentiation.[12, 47] The nucleus is a responder to external mechanical force, but the nucleus has only recently been understood as a mechanoresponsive organelle, potentially independent of cytoskeletal contributions. Therefore, to understand the nucleus' role in handling external forces, individual mechanisms and transduction processes must be understood.

Nuclear mechanics and morphology are important for dictating gene regulation. These properties are interrupted by human diseases like cancer, progeria, muscular dystrophy, and others.[32,50] Recently, it has been understood that Sun 1&2, Emerin, LaminA/C are directly tied into chromatin dynamics[12]. This study individually eliminated Sun 1&2, Emerin, and LaminA/C through small interfering RNA (siRNA). The depletion of each component resulted in two major findings: 1) increased spontaneous chromatin movement and 2) increased chromatin displacement under oscillatory loading, with the largest displacement resulting from depleting LaminA/C. This suggests that Sun, Emerin, and lamins play a role in chromatin function, with the key player being LaminA/C due to its direct connection. Additionally, research shows that LaminA/C and chromatin both play specific roles in force responses and preservation of the cell nucleus[7]. Nuclear

lamina elements Lamin A and Lamin C which exist in conjunction as LaminA/C, but not Lamin B1, has been shown to be an important contributor to nuclear stiffness[13]. It has been shown that LaminA/C levels are associated with stiffness by existing in relatively low concentrations in cells that are soft and high concentrations in cells that are stiff (Figure 2.).

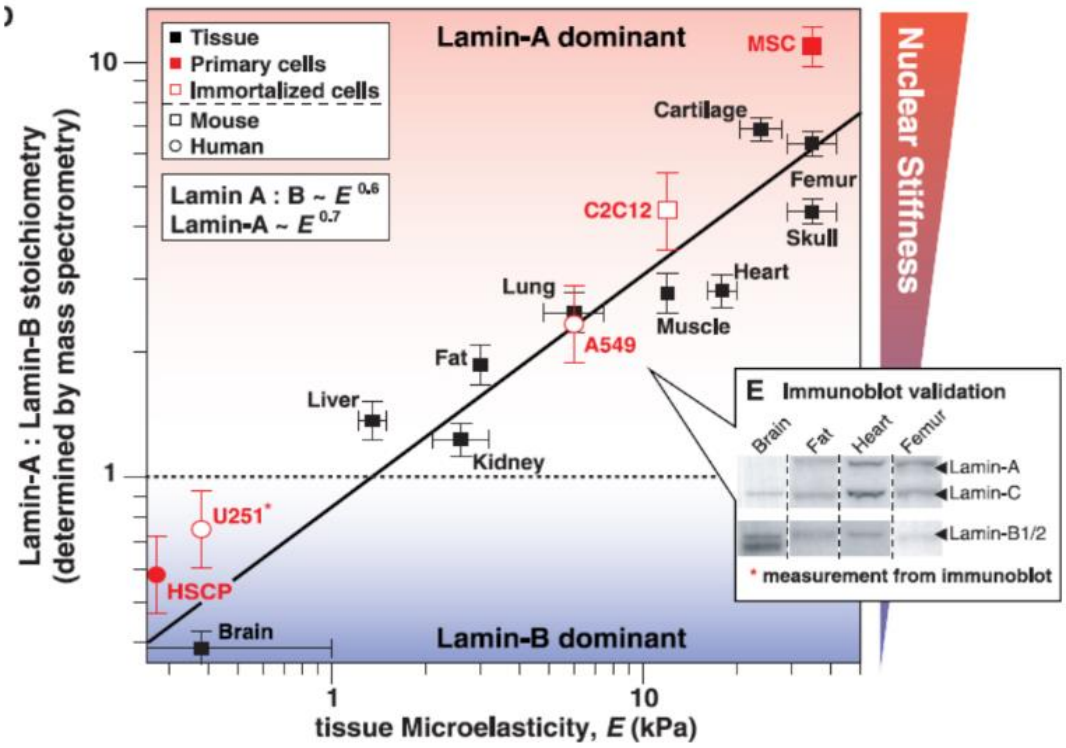

Figure 2. LaminA/C levels in varying tissues[13]

LaminA/C and nuclear stiffness also show to play roles in DNA regulation for cell health. One study showed that highly metastatic cancer cells were softer and presented relatively lower levels of LaminA/C when compared to healthy mammalian cells[32]. Since cancer cells are the results of improper functions of DNA, cell stiffening response to mechanical force must be properly regulated by LaminA/C. Nuclear LaminA/C's direct integration with Sun 1&2 proteins as well as other LINC components

has been shown to be the main player in harnessing cytoskeletal connections to shield nuclear morphology from mechanical deformation and block resultant damage[9]. Interestingly, co-depletion of LINC elements Sun-1 and Sun-2 from nuclear envelope also increases nuclear deformability[11]. Towards the interior of the nucleus, Lamin A/C has been shown to regulate and interact with chromatin dynamics.[16] Chromatin plays its own role in nuclear mechanics, independent of LaminA/C.[10]

Chromatin is a highly organized genetic structure, which consists of DNA tightly wrapped around histone proteins. These units of DNA and histones are known as nucleosomes. Nucleosomes are bound together to form chromatin chain-like structures. Chromatin directly binds to LaminA/C. Recently shown to play a role in mechanotransduction through small levels of displacement due to tension, chromatin is subject to influences through mechanical cues passed through LaminA/C. New found evidence has shown nuclear lamina to serve a purpose in two regions of the nucleus: the periphery (beneath the inner nuclear membrane) and throughout the interior of the nucleus (integrating throughout chromatin). Approximately sixty percent of the nuclear lamina in the form of LaminA/C exists in the periphery, while the other forty percent is believed to exist throughout chromatin regions and serves as a heavily integrated part of genomic regulation.[16] In fact, tension directly applied to the exterior of the cell, using magnetic twisting cytometry, causes chromatin stretching through lamina-chromatin interactions, directly corresponding to an upregulation of gene transcription.[12] In addition, LaminA/C and chromatin dictate force response of the nucleus under specific strain rates.[7] In whole nucleus small strain deformations (< 30% strain) chromatin showed to dominate mechanical regulation by increasing the spring constant 1.5-fold,

which was associated with changes in chromatin condensation with stiffening. When strain deformations are greater than 30% LaminA/C takes over in mechanoresponse. Here, LaminA/C provides an opposing force to tension that is up to 2.5 times greater than its resting state spring constant. Both LaminA/C and chromatin mechanisms show a team effort in resisting force to stretching, giving more traction to the idea of a self-protection method from rupture or other damage due to mechanical stretching. These findings also point to the importance of the nucleus in having its own mechanoadaptive system with LINC complex and lamina-chromatin interactions.

2.4.1 Chromatin condensation and nuclear stiffness are viewed as differentiation markers

Further research implies that nuclear morphology, stiffness, and chromatin morphology are indicators of MSC differentiation. Nuclear stiffening may be both a consequence and mediator of differentiation[51]. Here they measure that undifferentiated stem cells have less-stiff (more deformable) nucleus and lower cytoskeletal tension on the nucleus than differentiated nuclei. The differentiated nuclei showed stiffer nuclei, relocation of LaminA/C to the nuclear periphery, and higher heterochromatin condensation. Likewise, chromatin condensation is shown to increase with nuclear stiffness. [59] Additionally, chromatin condensation may be a marker for healthy or diseased cells, as it is shown that highly metastatic cancer cells have much lower chromatin condensation when compared to healthy cells. [32] This suggests that gene transcription is significantly upregulated leading to undesired cell function. Chromatin morphology, nuclear stiffness and architecture are markers of cell function and health.

2.5 MSC Response to Mechanical Loading

Mechanical forces influence stem cell dynamics, decisions, and lineage selections. Nuclear response to specific applied loads (magnitude, frequency, time interval) and mechanisms responsible are not well understood. MSCs are biomechanically responsive in the fact that mechanical signals regulate MSC actions through stiffness of external environment and application of external forces. For example, MSCs have shown variation in stiffness levels when cultured on substrates with varying rigidities, where MSCs increase in elastic modulus when cultured on stiffer substrates and vice versa.[31] Substrate stiffness in conjunction with altering nuclear structure through LaminA/C regulation is shown to influence MSC differentiation into osteocytes.[13] Here, 80% of MSCs that were subject to both a stiff matrix (40 kPa) and overexpression of LaminA/C (osteogenic conditions) were positive for osteogenic markers in ECM. Adipogenic conditions involved a softer matrix (0.3 kPa), where osteogenesis in MSCs was suppressed. Endogenous LaminA/C levels were naturally increased by 2-fold under osteogenic producing conditions, while levels were decreased under adipogenic conditions. This agrees with the evidence that mechanically stiffer tissues, being composed of cells with stiffer nuclei, result in (or are the result of) higher levels of LaminA/C. This also shows that the stiffness of the cell's environment in fact dictates its own stiffness through changes in nuclear mechanics.

Since MSCs exist an everchanging environment, researchers have developed several techniques to apply force and measure mechanoresponse and changes in cellular architecture. Popular methods include: applying mechanical strain to the ECM[18], micropipette aspiration to the cell and isolated nucleus[19], magnetic tweezers and beads

for applying tensile stress toe the ECM and nucleus[11], molecular beads to stretch or shear the nucleus directly[17], nanopillar arrayed platforms to measure cytoskeletal-generated force[20], and atomic force microscopy techniques to both apply compression measure mechanical properties of specific cellular components at both the micro and nanoscales.[21] Current research is limited to looking at nuclear adaptations either *in vitro* or *ex vivo*, typically not both. Newer research has focused on removal of the nucleus from the cell and applying direct mechanical force to the nuclear membrane, using techniques previously described. Two studies include applying tension and/or shear directly to Nesprin connections, that transfer force to the nucleoskeleton, imitating the cytoskeletal connections.[11,17] These studies applied either cyclic loading or static force in either tension or shear directly to the outer nuclear membrane. Both studies confirmed that the nucleus responded by increasing the resistance force generated by small transitions in the nucleoskeleton or decreased change in diameter after continual tension. This means that as the nucleus directly experiences force, it becomes more rigid, and less deformable, showing a force response independent from the rest of its cell.

While methods of mechanical application are established in triggering force response of the cell and isolated nucleus, it is unknown the exact mechanisms within the nucleus that are responsible for fate decisions and physiological changes as a result of such methods. While these cytoskeletal forces can be generated in multitude of ways, our group has been focused on Low Intensity Vibrations (LIV). LIV is a mechanical regime modeled after physiologic, high frequency muscle contractions[25,26] and in healthy MSCs, LIV promotes proliferation[24] and osteogenic differentiation leading to bone anabolism.[22] Low intensity vibration (LIV), or low magnitude high frequency vibration techniques,

compliant with safe levels of human exposure (0.3 – 1.0g, 30-90 (ISO-2631)) have been utilized in human and animal studies to show promotion of musculoskeletal anabolism, as a potential therapeutic option for osteoporotic or sarcopenic patients.[22] We reported LIV (0.7g, 90Hz) increases the phosphorylation of FAK at Tyr 397 and Akt at Ser 473 residues, resulting in increased GTP bound RhoA levels and robust F-actin bundling.[23] An interesting finding shows effects of LIV are additive, with a second bout of LIV increasing FAK phosphorylation and F-actin contractility due to either mechanical strain or RhoA activating agents like LysoPhosphatidic Acid.[6] When LIV is applied over a period of seven days, mRNA expression panels show significant increases in F-actin modulatory genes in LIV groups when compared to non-LIV controls.[24] These positive effects of LIV on actomyosin contractility translate into increased focal adhesions[23] and suggest that LIV will lead to greater force exerted on the nucleus through LINC complexes. While we have further reported that LIV applied daily increases stiffness of F-actin and results in increased mRNA expression of LINC-related genes Nesprin-1&2, Sun-1&2, and LaminA/C in MSCs, the role of LIV on nuclear remodeling and the mechanotransduction pathway is unknown.

Vibration is a complex method of force application directly to the exterior of the mesenchymal stem cell that exhibits a constant change in vertical direction, while introducing a variety of forces, which travel from focal adhesions, through the actin cytoskeleton and to the nucleus through the LINC complex[23]. The impact of LIV signals on both the nucleoskeleton, nuclear stiffness, and chromatin regions is not evident. Responsible mechanisms and specific biomechanical responses remain unclear. Therefore, ways of measuring effective nuclear response to LIV include: nuclear stiffness

measurements, levels of LaminA/C and Sun 1&2, morphological changes in the nuclear membrane, and changes in chromatin. Identifying key nuclear structures and changes in DNA morphology will provide more insight as to how the nucleus is regulated by LIV.

CHAPTER THREE: DEVELOPMENT OF RESEARCH METHODS AND PROTOCOLS

3.1 Defining Methods of Measurement

To effectively measure specific nuclear responses to LIV, clear measurement parameters must be defined. As mentioned in chapter two, the nucleus and MSC exhibit distinct individual responses when subjected to external stimuli.[17-20] The nucleus specifically responds to direct forces by creating an opposing force of its own[11]. However, the mechanisms responsible for this force are unclear. Therefore, to determine if LIV dictates a nuclear response, a clear marker is needed, such as measuring changes in stiffness of individual nuclei post-LIV stimulation. A change in nuclear stiffness has shown to be the result of tensile forces applied to the nucleoskeleton, through actin cytoskeleton polymerization, and further through Sun 1&2 of LINC complex and finally Lamin A/C, which resides at the periphery of the INM. Furthermore, to attribute a change in stiffness to specific structural components of the nucleoskeleton, Sun 1&2 and LaminA/C regulation must be measured as potential mechanisms responsible for change in nuclear structure. In congruence with changes in structural properties, nuclear morphological changes, involving the shape of the nucleus, influenced by attachments of the cytoskeleton, and chromatin condensation or decondensation should be analyzed, to evaluate chromatin's role and response to LIV. Force transferred from actin filaments, through Sun 1&2 and then to Lamin A/C have been shown to directly impact chromatin

condensation. Therefore, potential changes in regulation of Lamin A/C by LIV may contribute to dynamic alterations in chromatin.

Thus, in this chapter we will detail the methods, developed during this thesis, to measure nuclear response to LIV from analyzing mechanical properties, structure, and geometry of the nucleus, as outlined above.

3.2 Atomic Force Microscopy for Effective Stiffness Measurements

The first measurement criterion is to measure the mechanical stiffness of the MSC. The chosen technique to precisely measure the MSC stiffness, or elastic modulus, uses atomic force microscopy (AFM). The AFM employs a cantilevered probe, with a known spring constant. When the probe makes contact with the experimental sample, a laser, reflected off the back of the probe cantilever, is deflected, and measured by a position sensitive photodiode that records the location of the laser. In our experiments, following initial contact with the cell, the probe moves at a rate of 2μm/s for a total of one second, compressing and releasing the test sample (1μm approach, 1μm retract). The photodiode receives and records the displacement of the laser, resulting in a force-displacement curve. The AFM measurement process is illustrated in Figure 3.

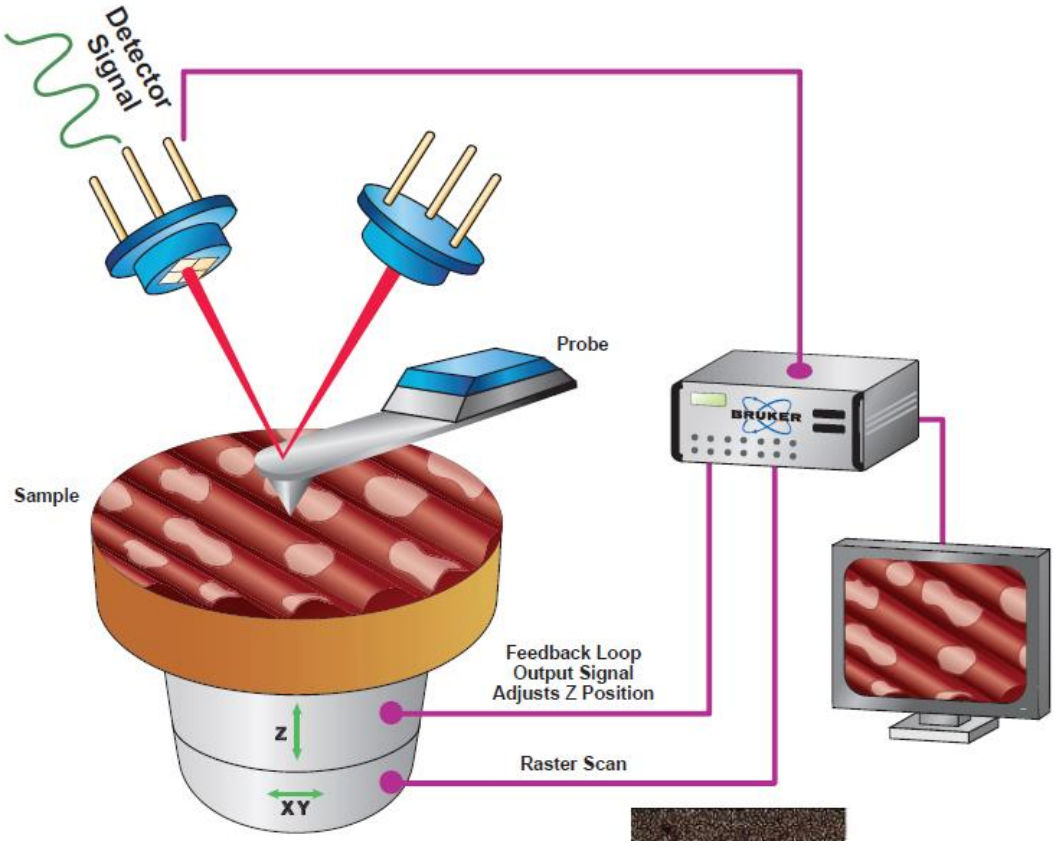

Figure 3. Atomic Force Microscopy Measurements[27]

The AFM, developed in 1986 for mapping the nanoscale topography of surfaces, has more recently incorporated nanomechanical property measurements of biological tissues, specifically measuring the Young's modulus. The Young's modulus, or elastic modulus, is a material's resistance to being deformed elastically. Elastic modulus (E) is the ratio of tensile stress to tensile strain along their corresponding planes. Current research testing the mechanical properties of biological tissue using AFM measurements involves a variety of cell types, fibrous tissues, and growth substrates. Our group tested two biological samples: MSCs *in vitro* and individual nuclei *ex vivo.* To accurately test these biological specimen, specific parameters were set for AFM measurements. The AFM tip has several options, which can be applied to a variety of materials with unique

mechanical parameters. For MSC measurements over the ellipsoid/spherical-like structure, which is the nucleus, the Hertzian spherical contact model can be applied.

The Hertzian model assumes contact between two spherical structures, which are subject to deformation and displacement. Therefore, the proper AFM tip when a Hertzian model is assumed is a spherical tip, as has been demonstrated in prior studies[28]. Here, we utilize a 10μm diameter spherical glass bead as the AFM probe tip. The Hertzian model also assumes relatively small displacements (indentation depth should be less than AFM tip radius[29]). The AFM indentation depth is 1μm and the AFM tip radius is 5μm. The AFM measures force versus displacement of both the test material and the AFM cantilever. The latter of the two is a known spring constant of 0.03N/m. The relationship of force to displacement, using the Hertzian model, can be determined using Equation 1.

Equation 1. Hertzian Force-Displacement Model

$$F = \frac{4\sqrt{R_c}\, E\, \delta^{\frac{3}{2}}}{3\,(1-\vartheta^2)}$$

where R_c, E, ϑ, and δ, are radius of curvature for AFM tip, elastic modulus, Poisson's ratio of the sample, and deflection, respectively. F, is the force required to displace the test sample a specific distance. Since F, R_c, δ, ϑ, are known, the elastic modulus of the sample remains the only unknown. The poisson's ratio, ϑ, is set at 0.5 for cells as it has been modeled under a soft incompressible and elastic biological material.[28] Our research used 0.3 for poisson's ratio, from the default setting of the Hertzian model applied on Bruker's Nanoscope software. The elastic modulus was calculated by rearranging the Hertzian mechanics contact equation (Eq. 2)

Equation 2. Hertzian Formula Rearrangement to Obtain Elastic Modulus

$$E = \frac{3F\ (1 - \vartheta^2)}{4\sqrt{R_c}\ \delta^{\frac{3}{2}}}$$

Force curves produced from AFM measurements were analyzed using Bruker's Nanoscope Analysis software and applying the Hertzian model. A contact point-based method was used to estimate the correlation value between the Hertzian curve and the experimentally obtained force curve. The point of contact was visually placed until the R^2 value for the Hertzian curve fit was greater than 0.95 ($p<0.05$), which then gives an accurate elastic modulus for each specific cellular component (Figure 4.). Each individual sample (i.e.., MSC or isolated nucleus) was subjected to three measurements, producing three force curves for each sample. The resulting values for elastic moduli were compared between samples using 0.3 and 0.5 for ϑ. The *E* values of samples using 0.5 showed to be 75% of the *E* values using the 0.3 poisson's ratio across all samples tested.

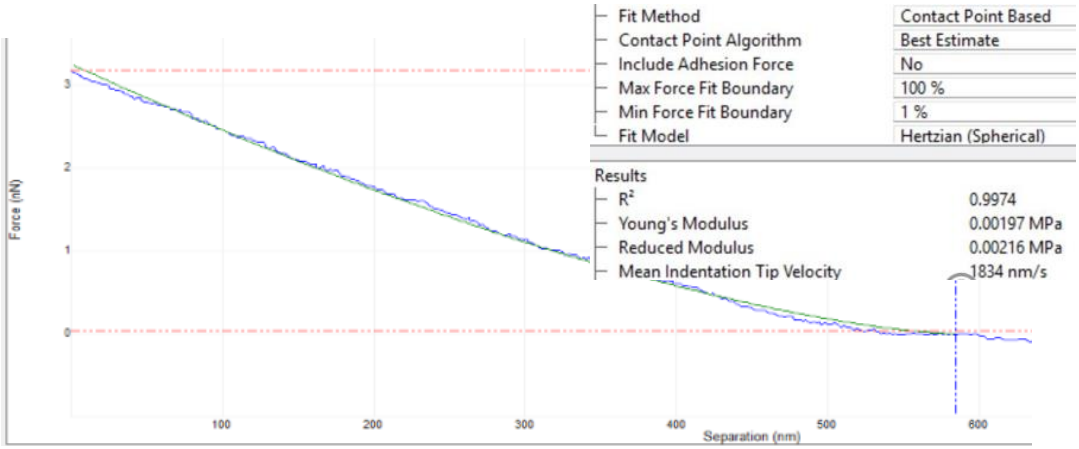

Figure 4. Nanoscope Force-Displacement Curve and Analysis Toolbox

Initial AFM experimentation involved developing a cellular testing protocol for elastic modulus. Isolated MSCs were individually selected for this process, where they

were measured over the center of the nucleus. *E* values were obtained and compared to current research,[58] using the Hertzian model and similar AFM techniques to acquire elastic modulus, ensure accuracy of testing. The next logical step involved testing individual nuclei isolated from the cell. This required a nuclear isolation protocol. Highlighted in chapter four, development of an isolation protocol involved diluting MSCs in a hypotonic buffer, which allowed clean nuclei to remain after centrifugation. Following several iterations, clean nuclei were plated on 35mm cell imaging plates for further analysis.

3.3 Evaluating Nuclear Survivability

The general procedure developed for AFM measurement of the elastic modulus of MSCs was rather simple. This involved cell culturing MSCs in 10% fetal calf serum and 1% antibiotic until 80-90% confluency was reached. Once proper confluency was reached, the cell medium was changed to phosphate-buffered saline (PBS) solution and AFM testing was conducted. Following multiple trials, an estimated completion period of 1 hour per ten samples was established. The nuclear isolation protocol involved a two-hour isolation protocol, including a thirty-minute period where nuclei, incubated at 37°C, attach to a poly-l-lysine coated cell culture dish. Immediately following complete attachment, nuclei were tested via AFM. Similar to the intact MSC, the testing interval for isolated nuclei was concluded at approximately one-hour after testing was initiated. After this protocol was developed into a consistent process, a question occurred: How long do isolated nuclei survive following isolation?

Testing nuclear survivability, following isolation, was a critical part in validating the current AFM testing protocol. A protocol that exposes the nucleus to a non-cell

environment (*ex vivo)*, resulting in nuclear death, would lead to invalidated results. However, it was unknown the amount of time that the nucleus can survive once removed from the cell. Therefore, two groups of nuclei were isolated and tested over separate time windows following isolation. The first group was tested immediately after the isolation protocol and ending at the one-hour time point (0 to 1-hour group). The second group began AFM testing at the 1-hour post-isolation time point and ended testing at the two-hour time point (1 to 2-hour group). The results indicated no change in stiffness values between groups, suggesting that nuclei can survive up to two hours post-isolation. A third group (2-3-hour post-isolation) showed over 6-fold increase in stiffness, indicative of dying nuclei.[58] For further measures, after two-hours post-isolation, fixation methods were analyzed, and elastic moduli of groups were compared. Fixation techniques involve addition of paraformaldehyde so that their properties are preserved for multiple days. Following nuclear isolation, samples were subject to either 2% Paraformaldehyde in PBS or untreated (control). AFM results showed a 6-fold increase in stiffness of the nuclei fixed in Paraformaldehyde solution. This suggests that fixation methods are not valid for AFM testing of elastic modulus.

3.4 Computational Measurements of Geometric Properties of Nuclei and Chromatin with Fluorescence Imaging

Once a mechanical property measurement technique (AFM measurements) was established, the next aim involved development of a technique to measure nuclear morphology of the following: nuclear area, sphericity, and chromatin condensation. A combination of nuclear isolation, fluorescence imaging, confocal imaging, Fiji Image J, and MATLAB analysis were used to quantify morphological values. Each group: intact

MSC and Isolated nuclei, was obtained, and stained with Hoechst 33342 vital dye (DAPI stain), which stains the DNA of each nucleus blue. For nuclear geometry, images were taken on a Leica confocal microscope at the Department of Veterans Affairs clinic in Boise, ID. Confocal imaging was parameterized to take 16 individual pictures along the horizontal plane. This produced a three-dimensional image of each sample. Images were analyzed in each plane of view, top (X-Y), side (X-Z), side (Y-Z) as shown in Figure 5. Circularity of each plane was averaged among planes for respective samples. Circularity is based on a scale from 0 to 1.0, where 0 is a straight line and 1.0 is a perfect circle. The circularity tool on Fiji Image J was utilized to measure circularity of confocal images in all three planes of measurement for individual samples.

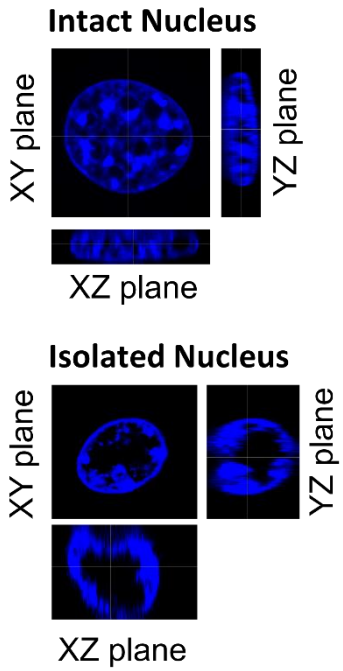

Figure 5. Confocal Images of MSC and Isolated Nuclei

Values for sphericity (an average of circularity values from three planes of imaging) were calculated on a scale from 0.0 being a plane, to 1.0 being a sphere. Averages showed

significantly higher sphericity in isolated nuclei (~0.8) in comparison to nuclei *in vivo* (~0.6). This main difference in sphericity occurred in the nuclear height between the two samples, with isolated nuclei doubling the height of nuclei *in vivo* (9.43μm vs 4.59μm, respectively). These results agree with current understandings that the nucleus exists under cytoskeletal tension while inside of the cell.[9]

Further analysis of nuclear membrane structural measurement involved disruption of key structural elements of the nucleus: LaminA/C, Sun-1, and Sun-2. To effectively measure the role of these individual elements, for both mechanical stiffness and effects on chromatin condensation, we utilized our newly developed AFM method and imaging techniques. Targeting specific LaminA/C and Sun-1&2 genes involved addition of small interfering RNA (siRNA) leading to individual knockdowns of each structure in the nuclear membrane. Following the five-day siRNA transfection protocol (highlighted in chapter 4, methods), MSCs were separated into six groups: control siRNA MSC, control siRNA nuclei (isolated), LaminA/C siRNA MSC, LaminA/C siRNA nuclei, Sun-1 and -2 siRNA MSC, and Sun-1 and -2 siRNA nuclei. Following group establishment, which involved a nuclear isolation protocol for "nuclei" groups, nuclei were either subject to AFM testing for elastic moduli measurements or stained with DAPI for imaging analysis. To identify the impact of depleting structural members on chromatin density, images of all siRNA and control groups took place on an ECHO Revolve epi-fluorescent microscope. Images were manually set to a constant brightness level and analyzed for nuclear area and chromatin condensation, using MATLAB scripts. The MATLAB program identified the periphery of the nucleus, developed a contrasted image, estimated chromatin, estimated number of nuclei, estimated centroids of nuclei, and black and

white image. Shown in Figure 6 are MATLAB images of a single nucleus. Values were estimated based on an intensity of pixels with a 30% higher intensity than background nucleoskeleton. Averages were computed for each of the six groups for 1) nuclear area, 2) chromatin/nuclear area and further 3) chromatin area per nuclear area. Since nuclei

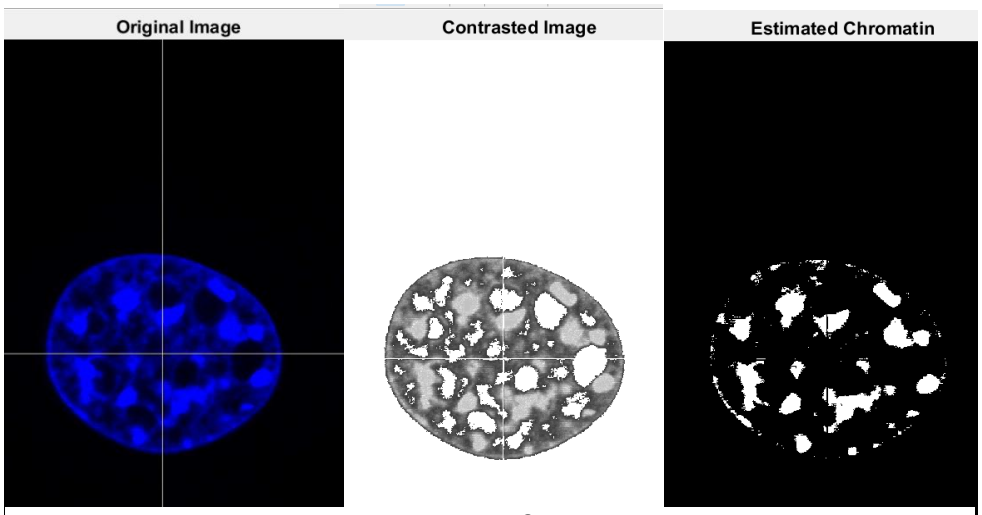

Figure 6. MATLAB Analysis of Nuclear Area and Chromatin Density

vary in size, relative chromatin levels were computed.

3.5 Development of an Effective Vibration Protocol for Mechanoresponse

The overarching experimental goal is to answer: how does the nucleus respond to mechanical stimuli delivered in the form of low intensity vibration? Based on our prior experimentation, a specific vibration intensity and frequency of vibration parameters were used (0.7g's, 90 Hz).[23] To trigger a response at a cellular level, MSCs were exposed to two twenty-minute vibration intervals, with a one-hour rest period in between vibrations, followed by another one-hour rest at the conclusion of the second and final vibration. Following this LIV, the MSCs were tested via AFM to evaluate a stiffening response. In the case of isolated nuclei, intact MSCs were subjected to the same protocol, then nuclei were isolated immediately following the last vibration interval and tested via AFM but showed no change in stiffness.

3.6 Measuring Nuclear Response to Low Intensity Vibration

An increased stimulus, to trigger a larger nuclear stiffness response was implemented through a "4x" LIV protocol (Figure 7). The reason behind doubling LIV to increase mechanoresponse is that effects of LIV have shown to be additive, by upregulating FAK phosphorylation, thus increasing F-actin contractility[6] then transferred

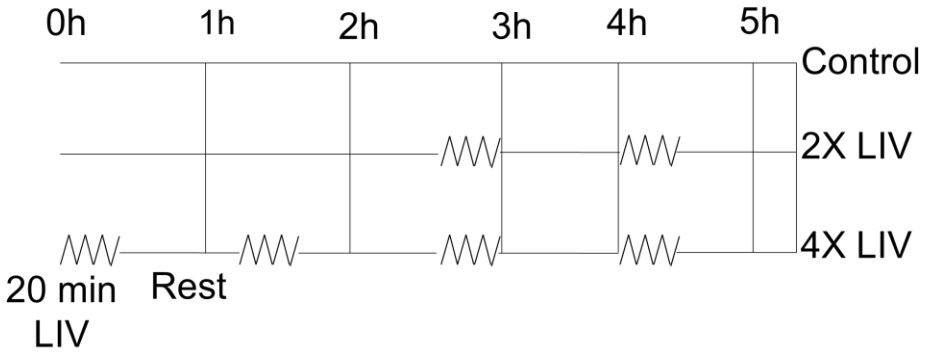

Figure 7. LIV Protocol Timeline: 2x vs 4x

to the nucleoskeleton. The 4x LIV protocol involved applying four periods of twenty-minute vibration with one-hour rests in between. After the conclusion of the fourth vibration, samples rested one more hour before they were subject to experimentation through: AFM testing, nuclear isolation, or fixation. Essentially, the 4x LIV protocol was doubling the LIV exposure of the original procedure, which is referred to as 2x LIV.

To further address our scientific question of the nucleus stiffening to LIV, we aimed to identify nuclear mechanisms responsible for changes in elastic modulus. LaminA/C, Sun-1&2, and chromatin were selected. Following 4x LIV, MSCs and Isolated nuclei were analyzed for changes in LaminA/C, Sun-1, and Sun-2 protein levels using a western blot protocol, which measures protein concentrations (Chapter 4, Methods). Following structural analysis of the nuclear membrane via western blotting, Further analysis included imaging 4x LIV samples and comparing nuclear area and chromatin condensation to controls. Using MATLAB scripts (Chapter 4, Methods) we

analyzed chromatin area per nuclear area and developed this into a ratio. The chromatin area/nuclear area ratio provides a value for chromatin condensation that is easily compared between samples. Since chromatin bundles cannot be larger than nuclear area, the ratio will always be between 0 and 1. A higher chromatin/nuclear area ratio indicates more chromatin decondensation and potentially upregulation in gene transcription.

CHAPTER FOUR: MANUSCRIPT. "ISOLATED NUCLEUS STIFFENS IN RESPONSE TO LOW INSTENSITY VIBRATION"

Newberg J[1], Schimpf J[2], Woods K[1], Losiate S[1], Davis P[2], Uzer G[1†]

[1]Mechanical and Biomedical Engineering, Boise State University

[2]Micron School of Material Science, Boise State University

† Corresponding Author

Running title: Isolated Nucleus Stiffens in Response to Low Intensity Vibration

Funding support: NIH P20GM109095, P20GM103408, 5P2CHD086843 and NASA NNX15AI04H

† Corresponding author:

Gunes Uzer PhD

Boise State University

Department of Mechanical & Biomedical Engineering

1910 University Drive, MSd-2085

Boise, ID 83725-2085

Ph. (208) 426-4461

Email: gunesuzer@boisestate.edu

4.1 ABSTRACT

The nucleus, central to all cellular activity, relies on both direct mechanical input and its molecular transducers to sense and respond to external stimuli. This occurs by regulating intra-nuclear organization that ultimately determines gene expression to control cell function and fate. It is long studied that signals propagate from an extracellular environment to the cytoskeleton and into nucleus (outside-in signaling) to regulate cell behavior. Emerging evidence, however, shows that both the cytoskeleton and nucleus have inherent abilities to sense and adapt to mechanical force, independent of each other. While it has shown that isolated nuclei can adapt to force directly *ex vivo*, the role of nuclear mechanoadaptation in response to physiologic forces *in vivo* remains unclear. To gain more knowledge on nuclear mechanoadaptation in cells, we have developed an atomic force microscopy (AFM) based experimental procedure to isolate live nuclei and specifically test whether nuclear stiffness increases following the application low intensity vibration (LIV) in mesenchymal stem cells (MSCs). Results indicated that Isolated nuclei, on average, were 67% softer when compared to intact MSCs ($p<.001$). In isolated nuclei, depleting LaminA/C and co-depleting Sun-1&2 led to 37% and 44% stiffness decrease as well as 47% and 39% larger chromatin area ($p<0.05$), respectively. When LIV was applied in series (0.7g, 90Hz, 20min) four times (4x), stiffness of isolated nuclei increased 66%. Changes in isolated nuclear stiffness was not accompanied by changes in LaminA/C or Sun1&2 protein levels, however chromatin area was 25% smaller in LIV treated nuclei compared to controls. Overall, stiffness of isolated nuclei increases with LIV as detected by AFM, and the effects on chromatin area suggests that LIV directly effects chromatin organization.

4.2 INTRODUCTION

Resident cells in tissues are subject multiple types of mechanical stimuli including, strain, fluid shear, compression, and forces due to acceleration. In response to these external stimuli, cells generate internal forces to maintain a homeostatic internal environment[30]. It has been long studied that forces, applied to the exterior of the cell at the ECM, propagate through the cell, via cytoskeletal components: focal adhesions and fibrous actin (F-actin) , and reach the structural components of the outer and inner nuclear membranes of the nucleus, which in turn regulates cell behavior, function, and fate[31].While changes in cytoskeletal compartment in response to mechanical challenge is well studied the changes that happen inside the nucleus in response to physiological forces is less understood.

Nuclei are mechanoresponsive organelles, integrated with cell structure through direct their connections with cytoskeletal elements.[14,15] When forces are applied directly to the nucleus *ex vivo*, resulting in strain deformations, nuclei stiffen through tyrosine phosphorylation of emerin,[11] suggesting that nucleus is an active contributor to mechanotransduction. Changes in the nuclear structure in turn influence gene transcription and cell differentiation.[12] It is understood that mechanical signals are converted into biophysical cues, within the cell, and control cell function and differentiation. For example, cells with higher elastic moduli are found in tissues with higher bulk stiffness[13] and in turn MSCs seeded into substrates with increasing stiffness, tend to differentiate into bone lineage[61] through regulation of LaminA/C and actin cytoskeleton.[33]

Nuclear stiffness is managed by number of structural elements, including structural components of the nuclear envelope, [14] cytoskeletal interactions, and chromatin.[15] Cytoskeletal elements connect directly to Nesprin proteins (Nepsrin1-4). [62] Nesprins are anchored to the inner nuclear membrane through Sun-1&2 proteins that directly interact with structural elements such as nuclear pore complexes and LaminA/C. Together Nesprins and Sun protein structures form the LINC complex[17] (Linker of Nucleoskeleton and Cytoskeleton). The LINC complex transfers force from the exterior of the cell to the intranuclear components.[36]. Current research has shown that Sun-1&2 and nuclear LaminA/C play key roles in structural integrity and mechanical regulation of the cell nucleus. LaminA/C binds directly to chromatin, which has shown to influence chromatin condensation, thus impacting nuclear decisions. [7] Chromatin has recently shown to play an independent role in nuclear mechanoresponse in coordination with LaminA/C as well. In this model, chromatin, modeled as a cross-linked polymer interior responds to small strain deformations of the nucleus (<30% strain) by independently increasing nuclear stiffness, while LaminA/C, understood as a polymeric shell, resists nuclear deformation for strains larger than 30%.[60]

Elastic modulus of cell nucleus can also be a marker of cell health. For example, it has been reported that nuclei of Hepatitis C-infected cells are significantly softer than healthy controls, which was paralleled by downregulation of LaminA/C nuclear proteins, but upregulation of β-actin.[34] Likewise, breast cancer cells exhibit large decreases in nuclear stiffness through similar mechanisms showing downregulations of LaminA/C and Sun-1&2[63]. Coinciding research showed chromatin decondensation as an additional component in highly metastatic cancer cells.[32] In a separate study, depletion of LINC

complex element Sun-1 or LaminA/C also resulted in significantly lower stiffness values of nuclei. [35]

Regarding dynamic mechanical signals, the nuclear envelope is subject to F-actin generated tension through LINC complex connections. [43] The nucleus responds to F-actin contractility by recruiting LINC complexes to apical stress fibers and leads to LaminA/C accumulation as well as changes in chromatin density under these stress fibers.[43] While, these cytoskeletal forces can be generated in multitude of ways, our group has been focused on low intensity vibrations (LIV). LIV is a mechanical regime modeled after physiologic, high frequency muscle contractions[38,39] and in healthy MSCs, LIV promotes proliferation and osteogenic differentiation[37]. We reported LIV increases the phosphorylation of Focal Adhesion Kinase (FAK) at Tyr 397 and Akt at Ser 473 residues, resulting in increased GTP bound RhoA levels and robust F-actin bundling.[6] The effects of LIV are additive, with a second bout of LIV augmenting FAK phosphorylation and F-actin contractility due to either mechanical strain or RhoA activating agents like LysoPhosphatidic Acid.[6] When LIV is applied over a period of 7 days, mRNA expression panels show significant increases in F-actin modulatory genes in LIV groups when compared to non-LIV controls, including RhoA stimulator ARHFGEF11 (Rho Guanine Nucleotide Exchange Factor 11, +6-fold) and Arp2/3 complex regulatory protein WAS (Wiskott-Aldrich syndrome, +43-fold).[5] These positive effects of LIV on actomyosin contractility translate into increased focal adhesions[6] and suggest that LIV will lead to greater force exerted on the nucleus through LINC complexes. While we have further reported that LIV applied daily increases stiffness of F-actin and results in increased mRNA expression of LINC-related genes Nesprin-1&2,

Sun-1&2, and LaminA/C in MSCs, role of LIV on nuclear structural properties is unknown.

Therefore, in these studies we utilized AFM based nanoindentation measurements, confocal imaging, and quantification of nuclear structural proteins to probe nuclear mechanical properties and morphology. We hypothesized that application of LIV to MSCs will increase nuclear stiffness.

4.3 METHODS

4.3.1 Cell culture

Primary mouse mesenchymal stem cells (MSCs) were extracted from bone marrow and tested for multipotentiality as previously described.[40,41] MSCs were selected because of their ability to differentiate into a multitude of cell types, typically adipocytes or osteocytes. MSCs between passage seven (P7) and P11 were used during experiments. For sub culturing cells were re-plated at the density of 1,800/cm^2 and maintained in IMDM (12440053, GIBGO) supplemented with 10% FCS (S11950H, Atlanta Biologicals) and 1% Pen/Strep. For whole cell experiments MSCs were plated into 35mm diameter dishes prior to application of LIV. For Nuclear extraction experiments cells were maintained in 55cm^2 culture dishes until 80% confluency (approximately 1.5 – 2 million cells) prior to application of LIV. Transfections and siRNA were applied 72h prior to isolation protocols.

4.3.2 Nuclear Isolation

MSCs were gently removed from plates by scraping in 9 mL of 1x PBS and centrifuged at 1100 RPM, 4^{o}C (Beckman Coulter Allegra X-30R). MSCs were then

gently suspended with 500µL hypotonic buffer A (.33M sucrose, 10mM HEPES, pH 7.4, 1mM MgCl2, 0.5% w/v Saponin) and centrifuged twice more at 3000 RPM, 4ºC for 10 minutes (Beckman Coulter Microfuge 20R Centrifuge). For western blots cytoplasmic fraction (supernatant) and nuclei (pellet) were saved separately. For AFM experiments cytoplasmic supernatant was aspirated and nuclei were resuspended in 100µL of hypotonic buffer A. To gently separate cytoplasmic debris from nuclei ,resuspended pellet was added onto 400µL of Percoll (Sigma Aldrich) + (81% w/v Percoll, Buffer A) and centrifuged at 10,000 RPM, 4ºC for 10 minutes, isolated nuclei were plated in a 0.01% poly-L-lysine coated 35mm cell culture dish and incubated for 25 minutes for proper adherence.

4.3.3 Overexpression and Small Interfering RNA (siRNA)

For transiently silencing specific genes, cells were transfected with gene-specific small interfering RNA (siRNA) or control siRNA (20 nM) using PepMute Plus transfection reagent (SignaGen Labs) according to manufacturer's instructions. Strain or LIV were applied 72 hours after initial transfection. The following Stealth Select siRNAs (Invitrogen) were used in this study: negative control for SUN-1 5′-GAAATCGAAGTACCTCGAGTGATAT -3′; SUN-1 5′-GAAAGGCTATGAATCCAGAGCTTAT-3′; negative control for SUN-2 5′-CACCAGAGGCTAGAACTCTTACTCA-3′; SUN-2 5′-CAACAUCCCUCAUGGGCCUAUUGUG-3′. ′; negative control for LaminA/C 5′-UGGGAGUCGGAAGAAGACUCGAUCA-3′; LaminA/C 5′-UGGGAGAGGCUAAGAAGCAGCUUCA-3′.

4.3.4 Force Application through Low Intensity Vibration Protocol

Vibrations were applied to MSCs at peak magnitudes of 0.7g at 90Hz for 20min at room temperature.[44] Controls were sham handled. LIV was applied as either 2X, two, twenty-minute vibration periods with one-hour rest in-between, or 4X, four twenty-minute periods, with one-hour rest between sessions. Following the last vibration, cells are then either subjected to nuclear isolation or analyzed via AFM or confocal imaging as intact cells.

4.3.5 Atomic Force Microscopy

Force measurements were acquired using a Bruker Dimension FastScan AFM. Tip less MLCT-D probes (0.03 N/m spring constant) were functionalized with 10 μm diameter borosilicate glass beads prior to AFM experiments. To ensure accurate force measurements, the probe's physical properties must be known. A thermal tune was conducted on each probe immediately prior to use to determine the spring constant and deflection sensitivity. MSCs and nuclei were located using the AFM's included optical microscope and engaged on with a low setpoint (2-3 nN) to minimize damage prior to testing. Three force-displacement curves were saved from each nucleus tested with at least 3 seconds of rest between conducting each test. Ramping was done at a rate of 2 μm/sec over 2 μm total travel (1 μm approach, 1 μm retract). Measurements that showed minimal contact with the nuclei were discarded and taken again to ensure an adequate depth of the structure was analyzed. The measured displacement produced force curves, which were then analyzed using Hertzian mechanics (spherical contact) [28,29,57] and Bruker's Nanoscope Analysis software to obtain elastic moduli of samples.

Measuring MSC and nuclear stiffness involved Bruker Atomic Force Microscopy, Nanoscope software, and excel. Force curves produced from AFM measurements were analyzed using Nanoscope software using a best-fit curve to a Hertzian (spherical) model. The point of initial contact was visually selected, and the curve was analyzed until the R^2 value was greater than 0.95 ($p<0.05$), which then gives an accurate elastic modulus to each specific cellular component. Each individual sample consisted of three measurements, producing three force curves. Averages for each sample were computed in excel. Averages for each group was then obtained, involving eight to twelve samples for each group using Microsoft Excel software. Outliers were then identified and rejected. Significance comparisons were made between stiffness values using independent t-tests between individual experimental groups at $p<0.05$.

4.3.6 Immunofluorescence and Image Analysis

Prior to experiments nuclei were stained with Hoechst 33342 vital dye (Nucblue, ThermoFisher) according to manufacturer instructions. Following LIV protocol, intact MSCs or isolated live nuclei were fixed with 2% paraformaldehyde for 15 minutes. For chromatin intensity analysis nuclei were imaged using an epi-fluorescence microscope (Revolve, Echo Labs). Chromatin intensity analysis were performed by a custom MATLAB script to select regions of nuclei. DAPI stain is used to define the regions of the nuclei through the use of blue channel. Each nucleus is individual defined along with its intensity. The mean brightness intensity of each nucleus is computed with chromatin being defined as +35 intensity of the average. The rest of the area is defined as non-chromatin. This was a more conservative definition of chromatin based on the test image.

The chromatin area and centroid are then defined using ‘region props’. The area and perimeter of the chromatin is output.

To quantify the nuclear geometry, using a Leica 6500 confocal microscope, entire height of individual cells or nuclei were imaged at intervals, which evenly divided each sample into sixteen vertical stacks. Confocal image stacks were imported into FIJI ImageJ software (https://imagej.nih.gov/ij/). Using Hoechst 33342 as a landmark, nuclear height was quantified via counting the number of stacks between first and last slices with detectable, in-focus Hoechst 33342 signal using cross-sectional images. Next, the entire nuclear section was collapsed into a single image using “Average Intensity Projection.” Nuclear area was measured via tracing the outer circumference of Hoechst 33342. This allowed for the perimeter in each of the three planes of measurement (XY, XZ, YZ) to be identified. From here, the “circularity” tool was used to compare each perimeter to a perfect circle. Averages for each plane of individual images were computed in excel for the two groups: intact MSC nucleus and isolated nucleus. The circularity values for each plane were averaged to obtain a sphericity value for the two groups of nuclei.

4.3.7 Western Blotting

Whole cell lysates were prepared using an radio immunoprecipitation assay (RIPA) lysis buffer (150mM NaCl, 50mM Tris HCl, 1mM EDTA, 0.24% sodium deoxycholate,1% Igepal, pH 7.5) to protect the samples from protein degradation NaF (25mM), Na3VO4 (2mM), aprotinin, leupeptin, pepstatin, and phenylmethylsulfonylfluoride (PMSF) were added to the lysis buffer. Whole cell lysates (20μg) were separated on 9% polyacrylamide gels and transferred to polyvinylidene difluoride (PVDF) membranes. Membranes were blocked with milk (5%, w/v) diluted in

Tris-buffered saline containing Tween20 (TBS-T, 0.05%). Blots were then incubated overnight at 4˚C with appropriate primary antibodies. Following primary antibody incubation, blots were washed and incubated with horseradish peroxidase-conjugated secondary antibody diluted at 1:5,000 (Cell Signaling) at RT for 1h. Chemiluminescence was detected with ECL plus (Amersham Biosciences, Piscataway, NJ). At least three separate experiments were used for densitometry analyses of western blots and densitometry was performed via NIH ImageJ software. Each blot was normalized to differences in control groups, using GAPDH or PARP, depending on protein molecular weight. Independent t-tests were then used to compare LIV groups to their respected control group at a significance level of $p<0.05$

4.3.8 Statistical Analysis

Results are expressed as mean ±standard error of the mean Statistical significance was evaluated by one-way ANOVA analysis of variance or t-test as appropriate (GraphPad Prism). All experiments were replicated at least three times to assure reproducibility

4.4 RESULTS

4.4.1 Cytoskeletal Tension Alters Nuclear Shape

We first investigated nuclear shape before and after nuclear isolation. Figure 8a shows intact MSC (top) and isolated nuclei (bottom) after DAPI staining. As shown in Fig.8a, isolated nuclei area were three times smaller than intact nuclei. Next, circularity of XY (top), XZ (side), YZ (side), were analyzed for intact MSC and isolated nuclei and combined to evaluate overall sphericity (Figure 8c). From a top view of the XY plane,

both intact and isolated nuclei showed no difference in circularity, but from both XZ and YZ planes, the isolated nucleus is 52% and 45% more circular than that of the intact MSC ($p<.001$ and $N=10$ for all groups), respectively. Combining the values of each plane, average circularity of the isolated nuclei was 0.809, which was significantly higher than the intact MSC nucleus (.612, $p<.001$). Measures of nuclear height and volume (figures 8.d & 8.e) showed that following nuclear isolation, height was increased by 105% and volume was decreased by 44% ($p<.001$ for both measurements).

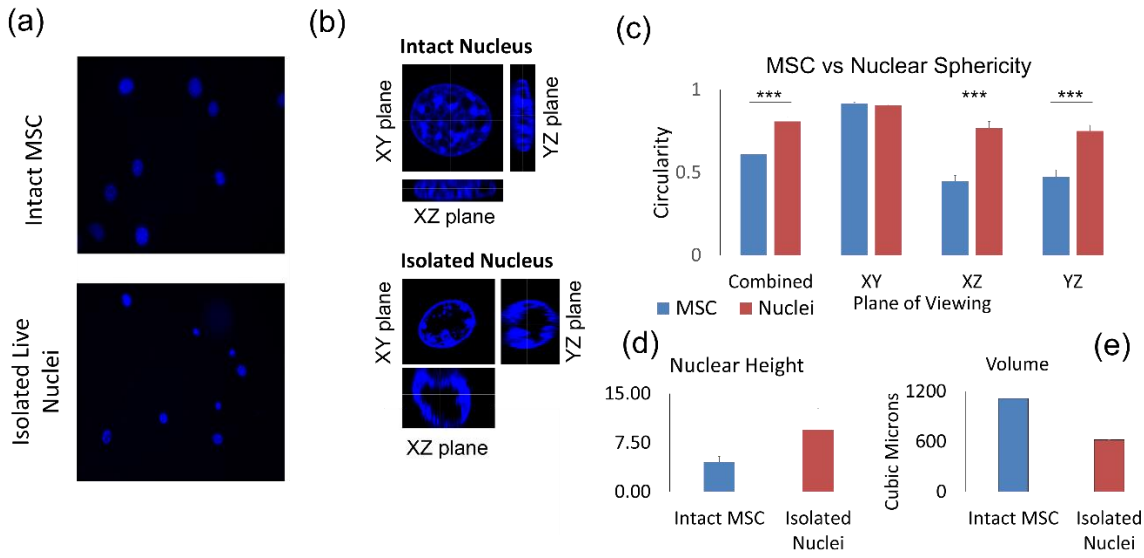

Figure 8. Cytoskeletal Tension Alters Nuclear Shape.

a) Mesenchymal stem cells and isolated nuclei (nuclear isolation protocol), were subjected to Hoechst 33342 and imaged for DNA under fluorescence microscopy. b) Confocal imaging of an intact nucleus and isolated nucleus with Hoechst 33342 fluorescence staining under 63X focus with 16 z-stacks for each image. Intact MSCs (top) and isolated nuclei (bottom) shown in XY, XZ, and YZ planes of focus. c) Shape profiles were compared between the intact MSC nucleus and isolated nucleus. The isolated and intact nuclei are similar in circularity from the XY plane but, show significant differences in shape profiles in XZ and YZ planes ($p<.001$, N=10 isolated nuclei, N=10 intact nuclei), with isolated nuclei showing 52% and 45% higher values for circularity respective to planes. The combined data, which is an average of all three planes, shows a significant difference in sphericity ($p<.001$) between the samples with the isolated nuclei and intact nuclei having sphericity values of 0.809 and 0.612, respectively. d) Isolated nuclear height (4.59µm) is approximately half of intact MSC nuclei (9.43µm). e) volume decreases from 1116µm^3 to 621µm^3 following isolation.

4.4.2 Nucleus significantly contributes to AFM-measured MSC Stiffness

To further investigate mechanical properties of the isolated nucleus, atomic force microscopy was implemented to obtain stiffness values (Fig.9a). First to test if we can use fixation methods to preserve nuclear stiffness, isolated nuclei were fixed in 2% paraformaldehyde and compared to untreated live controls. Shown in Fig.9c Results indicated a 4-fold increase in stiffness between paraformaldehyde and control isolated nuclei($p<.005$). We next tested the time-window by which stiffness of live cell nuclei remains stable. Using AFM, modulus of live, isolated nuclei were measured between a 0-1- hour span and a 1-2-hour span, following isolation (Fig. 9d). The figure indicates that no change occurred in the mechanical properties of isolated nuclei over a 2-hour testing interval, while there is a large spike in stiffness after 2 hours. This indicates that the 1-hour AFM testing window was safe. Next, we compared the stiffness of isolated vs intact MSC nucleus (tested on the center of the nucleus) within 1h of isolation. Shown in Fig.9e, isolated nuclei (1.72 kPa, N=53) were significantly softer than intact MSCs (2.48 kPa, N=45, $p<.05$). Therefore, the nucleus accounted for approximately 69% of the overall MSC stiffness.

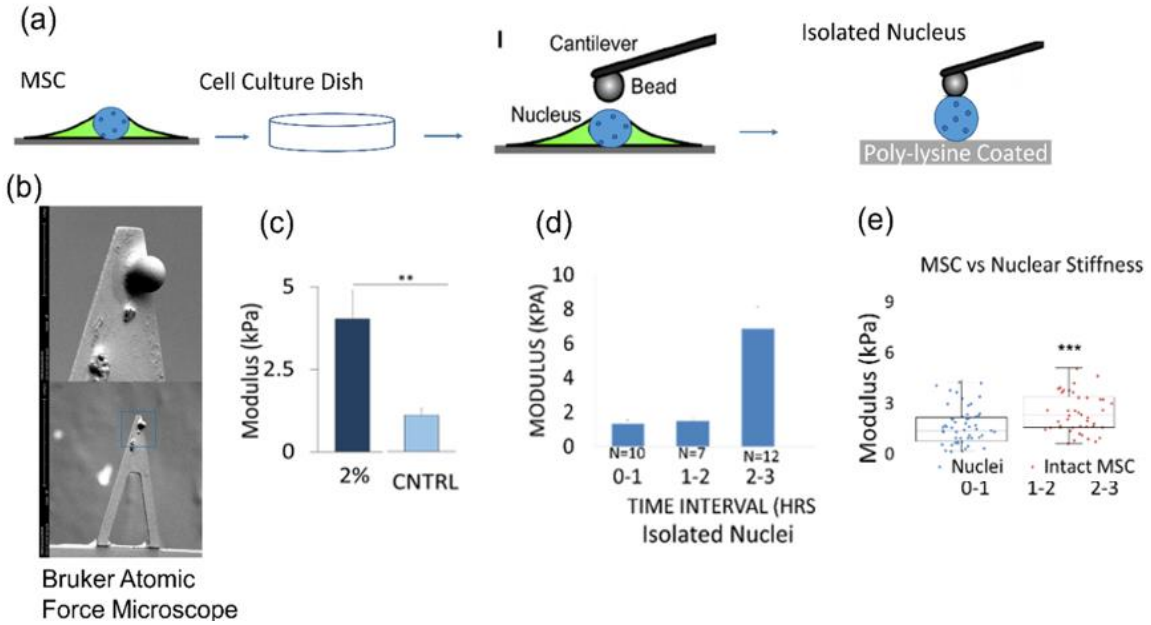

Figure 9. Nucleus significantly contributes to AFM-measured MSC Stiffness.

a) Nuclear isolation protocol involves plating of nuclei on 35mm cell culture dish coated in Poly-L-Lysine. Isolated nuclei are incubated for 25 minutes in 37˚C with 1mL 1X PBS for adhesion to substrate then subjected to AFM testing for up to 1 hour. b) Bruker atomic force microscope cantilever with attached bead. Images shown at 120μm (bottom image) and 20μm (top image). c) Fixation of isolated nuclei in 2% paraformaldehyde shows almost 4-fold increase in modulus when compared to control ($p<.005$, N=10 per group). d) AFM measurements show no change in the elastic modulus of isolated nuclei over a 2-hour testing interval. This indicates that the 1-hour AFM testing window is safe. e) Isolated nuclei are identified via AFM microscope and tested in the center of the nucleus to collect three individual measurements per sample. Intact MSC's and Isolated nuclei (both live) were plated on 35mm dishes and tested for stiffness via AFM for one-hour intervals. This figure includes several combined trials and shows that the cell nucleus makes up for ~69% of the MSC stiffness with a modulus of 1.72 kPa (N=53), while the remaining 31% resides in the cytoskeletal components. The average stiffness of MSCs passage 7-15 is 2.48 kPa (N=45).

4.4.3 Disruption of LaminA/C and Sun-1&2 decreases nuclear stiffness and changes structure

Further investigation into the structural properties of the nucleus targeted two known structural members in the nuclear membrane: LaminA/C and Sun 1&2 (Fig.10a). Following siRNA depletion of LaminA/C and Sun-1&2, groups were divided into either

intact MSCs or underwent a nuclear isolation protocol. Figure 10c shows significant decreases in stiffness between control and both LaminA/C and Sun-1&2 depleted samples for both isolated nuclei and intact MSCs. LaminA/C showed 66% and 37% decreases in stiffness in isolated nuclei ($p<.01$, $N=3$) and intact MSCs ($p<.005$, $N=10$), respectively. Likewise, siRNA against Sun-1&2 resulted in 77% and 44% decreases in modulus for isolated nuclei ($p<.01$, $N=5$) and intact MSCs ($p<.01$, $N=10$), respectively.

Hoechst staining of DNA can be used to identify heterochromatin. Therefore, using Hoechst 33342 and epifluorescence imaging, we quantified average heterochromatin size following LaminA/C or Sun-1&2 depletion. Shown in Figure 10d that nuclear area increased in LaminA/C siRNA MSC ($p<.001$, $N=73$), but not Sun-1&2 siRNA treated intact MSC ($N=55$). There were no differences in nuclear area between isolated nuclei subject to siRNA. A ratio of chromatin to nuclear area was next measured to compare possible heterochromatin condensation. Shown in Figure 10e, Sun-1&2 depletion increased in chromatin area to nuclear area ratio ($p<.01$ $N=55$), but not LaminA/C ($N=73$). Both siRNA against LaminA/C and Sun-1&2 show significantly larger ratios in isolated nuclei compared to controls ($p<.001$, $N=89$, $p<.001$, $N=92$, respectively).

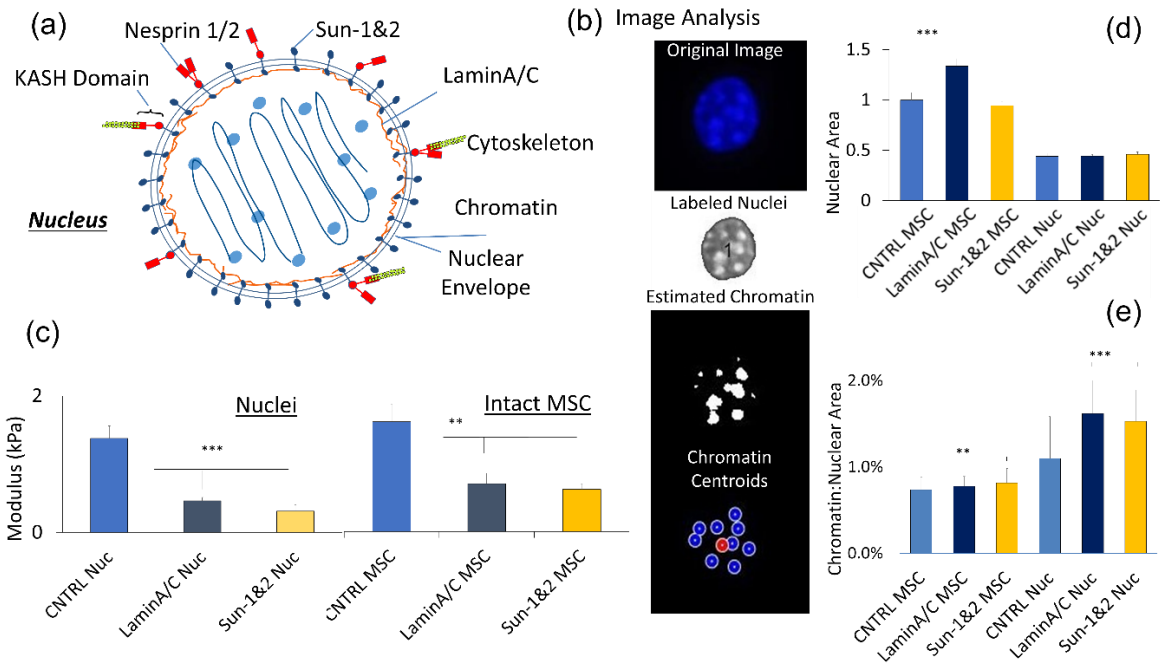

Figure 10. Disruption of LaminA/C and Sun-1&2 decreases nuclear stiffness and changes structure.

a) Representation of the nucleus with nucleoskeletal and cytoskeletal connection components illustrated including LaminA/C, Sun-1&2, Nesprin, and the KASH domain. b) MATLAB code was constructed to evaluate differences in nuclear area and nucleoli size as determined by live Hoechst 33342 staining. c) SiRNA against nuclear LaminA/C and Sun-1&2, significantly decreased both nuclear and intact MSC stiffness. For LaminA/C and SUN-1&2 depletion via siRNA, in isolated nuclei, elastic modulus decreased by 66% ($p<0.01$, N=3) and 77% ($p<0.005$, N=5), respectively. LaminA/C and Sun-1&2 depletion also showed significant decrease for intact MSC modulus by 37% ($p<0.01$, N=10) and 44% ($p<0.01$, N=10), respectively. d) Nuclear staining via Hoechst 33342 and epifluorescence imaging revealed that nuclear area was increased by 33% within intact MSCs subject to siRNA against LaminA/C ($p<0.001$, N=73) but not under Sun-1&2 depletion. Nuclear area had no significant changes within isolated nuclei control or experimental groups. e) Chromatin area to nuclear area ratios were calculated for all MSC and isolated nuclei groups subject to siRNA against LaminA/C and Sun-1&2. Intact MSC nuclei showed increased chromatin to nuclear area ratio for Sun-1&2 depleted nuclei ($p<.008$, N=55), but not LaminA/C depleted nuclei, compared to controls. Isolated nuclei showed significant increases in chromatin to nuclear area ratios for both LaminA/C ($p<.0001$, N=89) and Sun-1&2 ($p<.0001$, N=92) depleted nuclei compared to controls.

4.4.4 Low Intensity Vibration (LIV) stiffens MSC and Isolated Nucleus

To evaluate whether the nucleus responds to LIV we subjected intact MSCs to either 2x or 4x low intensity vibration protocols, which is illustrated in figure 11.a. Following 2x LIV, intact MSCs showed 71% increase in stiffness (fig. 11b), while there was no significant change in nuclear stiffness for isolated nuclei that underwent the same vibration protocol. Shown in figures 11b & 11c, application of 4x LIV increased nuclear elastic modulus in both intact MSCs (419% increase, $p<0.001$, $N=15$) and isolated nuclei (66%, $p<.05$, $N=10$).

Potential structural changes that corresponded with the changes in mechanical properties were evaluated via western blotting. LaminA/C and Sun-2 were probed in both the nucleus and cytoplasm to test whether vibration results in upregulation of either protein levels. These were then compared to PARP and GAPDH as control markers. Figure 11d shows that there are no significant differences in LaminA/C or Sun-2 proteins in cytoplasm or within the nucleus, following a 4X LIV protocol.

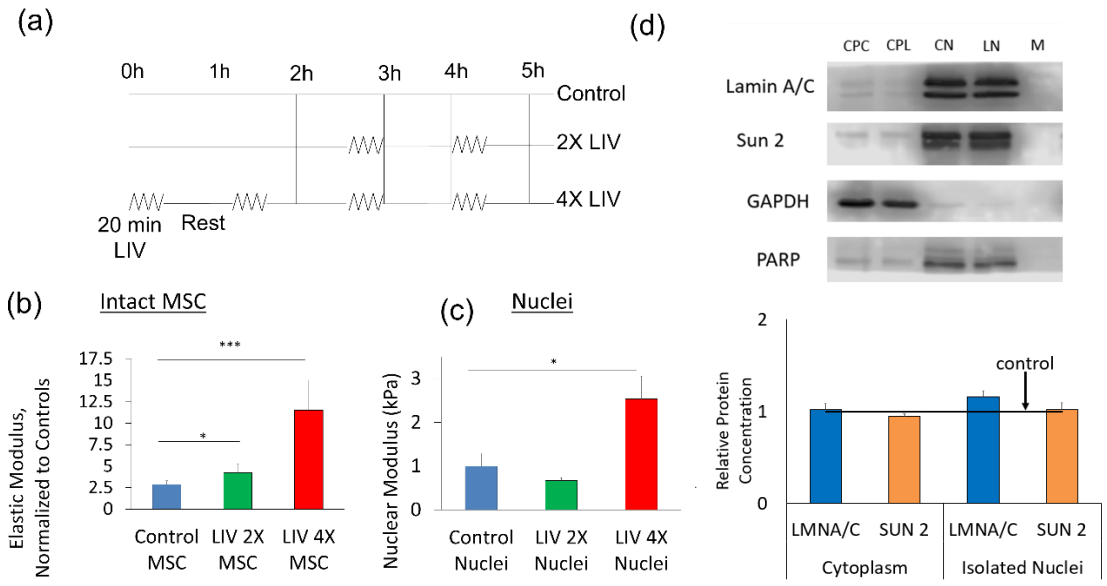

Figure 11. Low Intensity Vibration (LIV) Triggers Mechanoresponse in Both MSC and Isolated Nucleus by way of Stiffening.

a) Low intensity vibration (0.7g, 90 Hz) was applied to MSCs at twenty-minute intervals with one-hour rest in between each vibration period. 2X vibration included two, twenty-minute vibration periods, while 4X included four periods. b) 2X LIV on MSCs showed 71% increase (N=17, $p<0.05$). 4X LIV resulted in 4-fold increase in stiffness compared to control (N=15, 419% increase, $p<0.001$). c) Nuclear response to LIV was measured by applying the 2X LIV protocol to intact MSCs and then isolating nuclei to test stiffness. 2X LIV showed no significant increase (N=10) in stiffness in comparison to control (N=37). Nuclei responded to 4X LIV by showing a 66% increase in stiffness (N=10, $p<0.05$) when compared to control nuclei following post LIV isolation. d) Western blotting for Sun-1&2 and LaminA/C show no changes in levels for either Sun-2 or LaminA/C in 4x LIV groups compared to their respective controls.

4.4.5 Isolated Nuclei Maintain Heterochromatin Area after Vibration

As our findings showed increased heterochromatin area in LaminA/C and Sun-1&2 depleted nuclei, heterochromatin area was compared between 4x LIV and control samples for intact and isolated area (Fig12a,) Results show that intact MSCs subject to 4X LIV showed no difference nuclear area compared to controls (combined N=215, Fig 12.b). Likewise, there was no difference in nuclear area between isolated nuclei (combined N=96). Measuring heterochromatin area, intact MSCs subject to 4X LIV

showed no difference in chromatin to nuclear area ratio compared to controls (N=215). Isolated nuclei subject to 4X LIV showed a 25.4% lower chromatin to nuclear area ratio than isolated controls (p<.036, N=96).

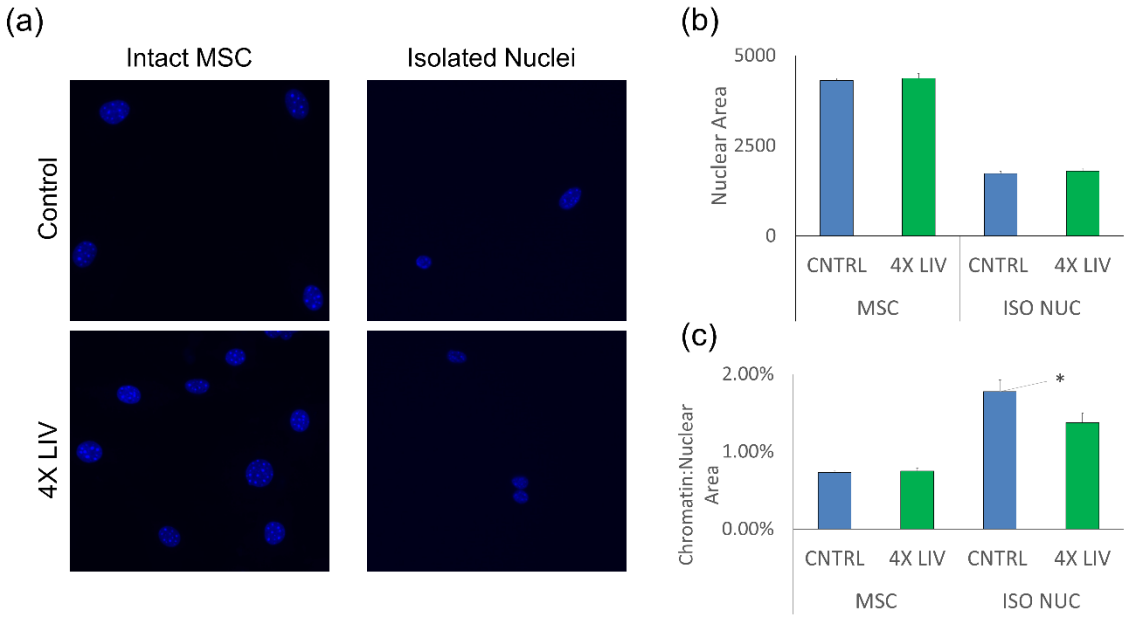

Figure 12. Isolated Nuclei Maintain Chromatin Density After LIV compared to Unloaded Controls.

a) Epi-fluorescence images of intact control MSC nuclei (upper left), Intact 4X LIV MSC nuclei (lower left), isolated control nuclei (upper right), and isolated 4X LIV nuclei (lower right). Cells were stained with Hoechst 33342 DAPI to stain heterochromatin and fixed in 4% Paraformaldehyde and 1% PBS for imaging. b) Nuclear area was measured using MATLAB code to identify nuclear bounds under DAPI staining. Intact MSCs subject to 4X LIV showed no difference in nuclear area compared to controls (N=215). There was no difference in nuclear area between isolated nuclei (N=96. c) Chromatin measurements were analyzed via MATLAB analysis. Individual chromatin were averaged and compared to respective nuclear area. Intact MSCs subject to 4X LIV showed no difference in chromatin to nuclear area ratio compared to controls (N=215). Isolated nuclei subject to 4X LIV showed a 25.4% lower chromatin to nuclear area ratio than isolated controls (p<.036, N=96)

4.5 DISCUSSION

In an environment consisting of continued and varying mechanical loads, it is evident that MSCs must mechanically adapt to their environments through motility, changes in structure, and differentiation[31]. Inability to properly adapt to the surrounding

environment due to mutations, that lead to softening of nuclear structure, like deficient LaminA/C levels, and decondensation of chromatin, are correlated with abnormal cells, including cancers[32] and inability to repair tissue due to laminopathies and myopathies. Our results here showed that the nucleus responds to low intensity vibration by way of stiffening, which is not due to an increase in LaminA/C or Sun protein amounts but instead, changes in the chromatin.

Here we investigated a low magnitude, low intensity vibration protocol on mesenchymal stem cell nuclei. Using confirming techniques such as: nuclear isolation, fluorescence imaging, siRNA against LaminA/C and Sun-1&2, and western blotting, we were able to identify visual structural changes in chromatin condensation and differences in mechanical stiffening of the nucleus using an atomic force microscopy technique. Combining these methods and statistical analyses we were able to conclude that the nucleus exists under tension within the cell, which changes its shape from 60% to 80% spherical after isolation. The increase in sphericity of the MSC nucleus following isolation suggests that there are external forces which forcefully elongate the outer nuclear membrane. The connection of fibrous actin to the nuclear membrane, recently established as the perinuclear actin cap, has shown to distribute force along the nuclear periphery.[42] However, the amount of stretching caused by the cytoskeleton and its impact on chromatin is unknown.

Given that there is a constant force on the nucleus, as it exists under cytoskeletal tension, abnormalities in nuclear architecture have shown to cause disease of many cell types. [50] Abnormally soft nuclei, due mainly to LaminA/C (but also Sun-1&2) deficiencies showed increased nuclear area from a top view. This finding points to a

weakening of nuclear structure and agrees with the current understanding that the cytoskeleton exhibits tension on the nucleus, causing even more nuclear stretching under LaminA/C depletion. Downstream of the mechanotransduction pathway, chromatin is directly impacted through connection to LaminA/C. Our research shows that chromatin area increases, in an intact MSC nucleus, under Sun-1&2 depletion. This disconnection of the nucleus from cytoskeletal connections shows to be an important regulator of chromatin structure. Following isolation, both LaminA/C and Sun-1&2 depleted nuclei show large increases in heterochromatin area, further suggesting that cytoskeletal connections to the nucleus influence heterochromatin organization. Chromatin structure and increase in area shows potential in upregulation of gene transcription as shown in research under direct nuclear stretching.[12] Therefore, softening of the nucleus, a tell-tale sign of abnormalities in the nucleoskeleton, may lead to changes in cellular decisions, functionality, and fate within a mechanical environment.

To target the nucleus as a mechanoresponsive element and specifically observe changes in mechanical properties, a low intensity vibration method was utilized. Vibratory signals influence bone development through cell proliferation and differentiation.[22] Here we evaluated whether low intensity vibration signals (0.7g, 90 Hz) had an impact on nuclear mechanoresponse. The results showed both a significant increase in stiffness for intact MSC nuclei and isolated nuclei, suggesting the nucleus responds to mechanical vibrations. Though the stiffness increased, there were no short-term changes in the levels of two major structural elements of the nucleoskeleton: LaminA/C and Sun-1&2. In addition, the stiffness of the isolated nucleus only increased 15% of the total increase in stiffness shown by that of the intact cell.

While we did not see changes in structural components, chromatin seemed to be impacted by LIV. In intact MSCs subject to 4x LIV, there was no difference in nuclear area or chromatin condensation. Following nuclear isolation, nuclei subject to a 4x LIV protocol showed significantly smaller, or more condensed heterochromatin. This finding shows that the effects of LIV were maintained by chromatin after the nucleus was mechanically separated from the cytoskeleton. This result may imply that LIV preserves DNA integrity due to abnormal mechanical loads on the cell nucleus. This increase chromatin condensation between isolated nuclei subject to LIV vs non-LIV counterparts, may contribute to the increased stiffening of the nuclei.

Until now, it was previously unknown whether nucleus independently responds to mechanical signals through low intensity vibration. Our research confirms that the nucleus is a mechanoresponsive element and responds to low intensity vibration by increasing its elastic modulus. The mechanisms responsible for this stiffness regulation are not fully known, but our findings suggests that chromatin structure may play a role in nuclear stiffening. Nuclear mechanical properties, like elastic modulus, have shown to be potential tell-tale signs of cell health, differentiation status, lineage decisions and now show to be influenced under a specific low intensity vibration protocol. Understanding the pathways which low intensity vibration and other forms of mechanical signal travel to the nucleus, causing changes in stiffness, nucleoskeletal structure, chromatin structure, and potential changes in gene regulation may serve a purpose in reviving abnormal cell mechanical function and potentially guiding MSC fate.

CHAPTER FIVE: SUMMARY AND FUTURE WORK

5.1 Summary of Current Research

Mesenchymal stem cells are responsible for the creation of all cell types, creating all tissues, in mammals. Human health and longevity rely on proper function of MSCs through correct differentiation and proliferation processes. MSCs respond to their external mechanical environment through changing their own internal mechanical properties. This mechanotransduction process transfers forces from the exterior to the interior of the cell, reaching the cell's nucleus and directly influencing gene regulation and MSC lineage decisions. Though it is known that MSCs respond to their mechanical environment, it remains unknown how the nucleus responds to mechanical signals *in vivo.* Therefore, we utilized low intensity vibration, which is shown to influence osteogenic differentiation of MSCs to address our hypothesis: Low intensity vibration applied to MSCs will increase nuclear stiffness.

The overarching experimental goals of this research were to:

1) Identify if the nucleus responds to low intensity vibration
2) Measure nuclear response to low intensity vibration via elastic modulus
3) Identify structural members of the nucleus responsible for stiffening response to LIV.

Experimental goals were achieved through utilization of the following techniques and protocols:

- Applying mechanical stimulus to mesenchymal stem cells through the form of LIV.
- Development of a nuclear isolation protocol to target individual nuclei *ex vivo* and evaluating nuclear survivability
- Utilizing atomic force microscopy techniques to measure elastic moduli of intact MSCs and isolated nuclei
- Development of a LIV protocol that triggered nuclear mechanoresponse in the form of stiffening
- Identification of changes in nuclear membrane proteins through an existing western blot protocol
- Analyzing nuclear morphological changes and chromatin changes through fluorescence imaging techniques, MATLAB, and Fiji image J analysis.

5.2 Key Results and Limitations

Through several iterations of previously mentioned experimental techniques and protocols, we have found that nuclei respond to mechanical stimuli, in the form of LIV, by way of stiffening. The specific results show that intact MSCs respond to four intervals of twenty-minute vibration (4X LIV) by increasing their stiffness four-fold, while the isolated nuclei increase by 66% under the same protocol. We aimed to identify nuclear components that contributed to the stiffening response by measuring changes in two key structural proteins, LaminA/C and Sun-1&2. Neither LIV stimulated MSCs nor

respective isolated nuclei groups showed change in LaminA/C or Sun-2 proteins. This suggests that protein levels in the nuclear membrane remain stable, but this does not exclude the idea of structural reorganization of such proteins. For example, it was shown that both changes in LaminA/C organization and chromatin condensation are associated with nuclear stiffness, following differentiation[51]. Therefore, a limitation and future direction of current research may be to identify reorganization of the nucleoskeleton following 4x LIV.

Furthermore, findings of this study showed that chromatin dynamics were impacted following LIV. Since the isolation protocol involves mechanical removal of the nucleus from its cytoskeletal attachments, it experiences mechanical disruption. This disruption is evident through a large increase in chromatin decondensation in isolated nuclei compared to intact MSC nuclei. Interestingly, isolated nuclei that experienced 4x LIV showed a significantly lower chromatin decondensation than non-LIV isolated nuclei. This may suggest that LIV protects DNA against mechanical damage through an increase in chromatin condensation. Since chromatin dynamics and nuclear membrane structure, such as LaminA/C, are directly tied-in together, these findings suggests that there may be changes in formation of the nucleoskeleton rather than the protein levels themselves. Although it is evident that cytoskeletal attachments to the nucleoskeleton plays a significant role in the increase of nuclear stiffness, *in vivo,* the fact that the nucleus stiffens in response to vibration, following isolation, suggests that there are changes in the nuclear structure, potentially due to chromatin condensation, which manages these mechanical characteristics.

5.3 Future Directions

The nucleus responds uniquely to various mechanical stimuli. This response includes changes in cellular and nuclear architecture, corresponding stiffness regulation, and overall gene expression. We have affirmed that the nucleus stiffens in response to LIV. Protein levels of structural elements (LaminA/C, Sun proteins) in the nucleoskeleton may not be in control of nuclear response to LIV, in the form of stiffening, instead their re-configuration along with chromatin dynamics look to be responsible for the changes in stiffness. Furthermore, we continue to investigate the exact mechanotransduction pathway of the LIV to the nucleoskeleton, the importance of the cytoskeleton in this regulation, and the specific impacts throughout the core of the nucleus; the DNA. Identifying the mechanotransduction pathway of specific applied force, and specific nuclear response can give insight to how force regulates the nucleus, gene regulation, and overall cellular decisions. The ability to quantify external loads on the deformation of the nucleus and associating this nuclear deformation with specific gene regulation, through understanding chromatin dynamics, would be breakthrough technology in therapuetical methods of applying specific forces to control cell fate.

REFERENCES

1. Stem Cell Basics IV. (n.d.). Retrieved from https://stemcells.nih.gov/info/basics/4.htm.

2. Stavenschi, E., Labour, M. N., & Hoey, D. A. (2017). Oscillatory fluid flow induces the osteogenic lineage commitment of mesenchymal stem cells: The effect of shear stress magnitude, frequency, and duration. *Journal of Biomechanics, 55*, 99–106. https://doi.org/10.1016/j.jbiomech.2017.02.002

3. Ren, L., Yang, P., Wang, Z., Zhang, J., Ding, C., & Shang, P. (2015). Biomechanical and biophysical environment of bone from the macroscopic to the pericellular and molecular level. *Journal of the Mechanical Behavior of Biomedical Materials, 50*, 104–122. https://doi.org/10.1016/j.jmbbm.2015.04.021

4. Legerstee, K., Geverts, B., Slotman, J., Houtsmuller, A. (2019) Dynamics and distribution of paxillin, vinculin, zyxin and VASP depend on focal adhesion location and orientation

5. Harris, A. R., Jreij, P., & Fletcher, D. A. (2018). Mechanotransduction by the Actin Cytoskeleton: Converting Mechanical Stimuli into Biochemical Signals. *Annual Review of Biophysics, 47*(1), 617–631. https://doi.org/10.1146/annurev-biophys-070816-033547

6. Gerlitz, G., Bustin, M. (2010) The role of chromatin structure in cell migration. *Trends in Cell Biology, 21(1),* 6-11.

7. Stephens, A. D., Banigan, E. J., & Marko, J. F. (2018). Separate roles for chromatin and lamins in nuclear mechanics. *Nucleus (Austin, Tex.), 9*(1), 119–124. doi:10.1080/19491034.2017.1414118

8. Klein-Nulend J, Bacabac RG, Mullender MG: Mechanobiology of bone tissue. *Pathol Biol [Paris]* 53:576–580, 2005.

9. Kim, J. K., Louhghalam, A., Lee, G., Schafer, B. W., Wirtz, D., & Kim, D. H. (2017). Nuclear lamin A/C harnesses the perinuclear apical actin cables to protect nuclear morphology. *Nature Communications*, *8*(1), 1–13. https://doi.org/10.1038/s41467-017-02217-5

10. Schreiner, S. M., Koo, P. K., Zhao, Y., Mochrie, S. G., & King, M. C. (2015). The tethering of chromatin to the nuclear envelope supports nuclear mechanics. *Nature communications*, *6*, 7159. doi:10.1038/ncomms8159

11. Guilluy, C., Osborne, L. D., Van Landeghem, L., Sharek, L., Superfine, R., Garcia-Mata, R., & Burridge, K. (2014). Isolated nuclei adapt to force and reveal a mechanotransduction pathway in the nucleus. *Nature Cell Biology*, *16*, 376. Retrieved from http://dx.doi.org/10.1038/ncb2927

12. Tajik, A., Zhang, Y., Wei, F., Sun, J., Jia, Q., Zhou, W., … Wang, N. (2016). Transcription upregulation via force-induced direct stretching of chromatin. *Nature Materials*, *15*(12), 1287–1296. https://doi.org/10.1038/nmat4729

13. Swift, J., Ivanovska, I. L., Buxboim, A., Harada, T., Dingal, P. C., Pinter, J., … Discher, D. E. (2013). Nuclear lamin-A scales with tissue stiffness and enhances matrix-directed differentiation. *Science (New York, N.Y.)*, *341*(6149), 1240104. doi:10.1126/science.1240104

14. Maurer, M., & Lammerding, J. (2019). The Driving Force: Nuclear Mechanotransduction in Cellular Function, Fate, and Disease. *Annual Review of Biomedical Engineering*, *21*(1), 443–468. https://doi.org/10.1146/annurev-bioeng-060418-052139

15. Miroshnikova, Y. A., Nava, M. M., & Wickström, S. A. (2017). Emerging roles of mechanical forces in chromatin regulation. *Journal of Cell Science*, *130*(14), 2243–2250. https://doi.org/10.1242/jcs.202192

16. Bronshtein, I., Kepten, E., Kanter, I., Berezin, S., Lindner, M., Redwood, A. B., … Garini, Y. (2015). Loss of lamin A function increases chromatin dynamics in the nuclear interior. *Nature Communications*, *6*. https://doi.org/10.1038/ncomms9044

17. Balikov, D. A., Brady, S. K., Ko, U. H., Shin, J. H., de Pereda, J. M., Sonnenberg, A., … Lang, M. J. (2017). The nesprin-cytoskeleton interface probed directly on single nuclei is a mechanically rich system. *Nucleus*, *8*(5), 534–547. https://doi.org/10.1080/19491034.2017.1322237

18. Guo, Y., Zhang, C. Q., Zeng, Q. C., Li, R. X., Liu, L., Hao, Q. X., … Yan, Y. X. (2012). Mechanical strain promotes osteoblast ECM formation and improves its osteoinductive potential. *Biomedical engineering online*, *11*, 80. doi:10.1186/1475-925X-11-80

19. Lele, T. P., Dickinson, R. B., & Gundersen, G. G. (2018). Mechanical principles of nuclear shaping and positioning. *The Journal of Cell Biology*, *217*(10), 3330–3342. https://doi.org/10.1083/jcb.201804052

20. Shiu, J. Y., Aires, L., Lin, Z., & Vogel, V. (2018). Nanopillar force measurements reveal actin-cap-mediated YAP mechanotransduction. *Nature Cell Biology*, *20*(3), 262–271. https://doi.org/10.1038/s41556-017-0030-y

21. González-Cruz, R. D., Fonseca, V. C., & Darling, E. M. (2012). Cellular mechanical properties reflect the differentiation potential of adipose-derived mesenchymal stem cells. *Proceedings of the National Academy of Sciences of the United States of America*, *109*(24). https://doi.org/10.1073/pnas.1120349109

22. Xie, L., Rubin, C., & Judex, S. (2008). Enhancement of the adolescent murine musculoskeletal system using low-level mechanical vibrations. *Journal of Applied Physiology*, *104*(4), 1056–1062. https://doi.org/10.1152/japplphysiol.00764.2007

23. Uzer, G., Thompson, W. R., Sen, B., Xie, Z., Yen, S. S., Miller, S., … Rubin, J. (2015). Cell mechanosensitivity to extremely low-magnitude signals is enabled by a LINCed nucleus. *Stem Cells*, *33*(6), 2063–2076. https://doi.org/10.1002/stem.2004

24. Uzer, G., Pongkitwitoon, S., Ete Chan, M. & Judex, S. (2013) Vibration induced osteogenic commitment of mesenchymal stem cells is enhanced by cytoskeletal remodeling but not fluid shear. *Journal of biomechanics* **46**, 2296-2302, doi:10.1016/j.jbiomech.2013.06.008.

25. Rubin, C., Xu, G. & Judex, S. (2001) The anabolic activity of bone tissue, suppressed by disuse, is normalized by brief exposure to extremely low-magnitude mechanical stimuli. *The FASEB Journal* **15**, 2225-2229, doi:10.1096/fj.01-0166com

26. Huang, Robert P., Rubin, C. T. & McLeod, K. J. (1999) Changes in Postural Muscle Dynamics as a Function of Age. *The Journals of Gerontology Series A: Biological Sciences and Medical Sciences* **54**, B352-B357, doi:10.1093/gerona/54.8.B352

27. AFM Microscopes - Introduction to Atomic Force Microscopy: Bruker. (2018, December 12). Retrieved from https://www.bruker.com/products/surface-and-dimensional-analysis/atomic-force-microscopes/campaigns/afm-microscopes.html.

28. Guo, Q., Xia, Y., Sandig, M., & Yang, J. (2012). Characterization of cell elasticity correlated with cell morphology by atomic force microscope. *Journal of Biomechanics*, *45*(2), 304–309. https://doi.org/10.1016/j.jbiomech.2011.10.031

29. Hertz, T. (n.d.). *Jpk-App-Elastic-Modulus.14-1 (1)*. 1–9.

30. Vining, K. H., & Mooney, D. J. (2017). Mechanical forces direct stem cell behaviour in development and regeneration. *Nature reviews. Molecular cell biology*, *18*(12), 728–742. doi:10.1038/nrm.2017.108

31. Martins, R., Finan, J., Guilak, F., Lee, D., 2012. Mechanical Regulation of Nuclear Structure and Function. *Annual Review of Biomedical Engineering, 14:431-55.*

32. Khan, Z. S., Santos, J. M., & Hussain, F. (2018). Aggressive prostate cancer cell nuclei have reduced stiffness. *Biomicrofluidics*, *12*(1). https://doi.org/10.1063/1.5019728

33. Buxboim, A., Swift, J., Irianto, J., Spinler, K. R., Dingal, P. C. D. P., Athirasala, A., … Discher, D. E. (2014). Matrix elasticity regulates lamin-A,C phosphorylation and turnover with feedback to actomyosin. *Current Biology*, *24*(16), 1909–1917. https://doi.org/10.1016/j.cub.2014.07.001

34. Balakrishnan, S., Mathad, S. S., Sharma, G., Raju, S. R., Reddy, U. B., & Das, S. (2019). Article A Nondimensional Model Reveals Alterations in Nuclear Mechanics upon Hepatitis C Virus Replication. *Biophysj*, *116*(7), 1328–1339. https://doi.org/10.1016/j.bpj.2019.02.013

35. Liu, L., Luo, Q., Sun, J., Song, G., (2019) Cytoskeletal control of nuclear morphology and stiffness are required for OPN-induced bone marrow-derived mesenchymal stem cell migration. *Biochemical Cell Biology*.

36. Arsenovic, P. T. *et al.* Nesprin-2G, a Component of the Nuclear LINC Complex, Is Subject to Myosin-Dependent Tension. *Biophysical journal* **110**, 34-43, doi:10.1016/j.bpj.2015.11.014 (2016).

37. Uzer, G., Pongkitwitoon, S., Ete Chan, M. & Judex, S. Vibration induced osteogenic commitment of mesenchymal stem cells is enhanced by cytoskeletal remodeling but not fluid shear. *Journal of biomechanics* **46**, 2296-2302, doi:10.1016/j.jbiomech.2013.06.008 (2013).

38. Rubin, C., Xu, G. & Judex, S. The anabolic activity of bone tissue, suppressed by disuse, is normalized by brief exposure to extremely low-magnitude mechanical stimuli. *The FASEB Journal* **15**, 2225-2229, doi:10.1096/fj.01-0166com (2001).

39. Huang, Robert P., Rubin, C. T. & McLeod, K. J. Changes in Postural Muscle Dynamics as a Function of Age. *The Journals of Gerontology Series A: Biological Sciences and Medical Sciences* **54**, B352-B357, doi:10.1093/gerona/54.8.B352 (1999).

40. Peister, A. *et al.* Adult stem cells from bone marrow (MSCs) isolated from different strains of inbred mice vary in surface epitopes, rates of proliferation, and differentiation potential. *Blood* **103**, 1662-1668, doi:10.1182/blood-2003-09-3070 (2004).

41. Case, N. *et al.* Mechanical activation of β-catenin regulates phenotype in adult murine marrow-derived mesenchymal stem cells. *Journal of Orthopaedic Research* **28**, 1531-1538, doi:10.1002/jor.21156 (2010).

42. Shiu, J. Y., Aires, L., Lin, Z., & Vogel, V. (2018). Nanopillar force measurements reveal actin-cap-mediated YAP mechanotransduction. *Nature Cell Biology*, *20*(3), 262–271. https://doi.org/10.1038/s41556-017-0030-y

43. Versaevel, M. *et al.* Super-resolution microscopy reveals LINC complex recruitment at nuclear indentation sites. *Sci. Rep.* **4**, doi:10.1038/srep07362

44. Sen, B. *et al.* Mechanical signal influence on mesenchymal stem cell fate is enhanced by incorporation of refractory periods into the loading regimen. *Journal of biomechanics* **44**, 593-599, doi:10.1016/j.jbiomech.2010.11.022 (2011).

45. Lammerding, J. *et al.* Lamin A/C deficiency causes defective nuclear mechanics and mechanotransduction. *The Journal of Clinical Investigation* **113**, 370-378, doi:10.1172/JCI19670 (2004).

46. Hematti, P. (2010). *Human Embryonic Stem Cell-Derived Mesenchymal Progenitors: An Overview. Embryonic Stem Cell Therapy for Osteo-Degenerative Diseases, 163–174.* doi:10.1007/978-1-60761-962-8_11

47. Le, H. Q., Ghatak, S., Yeung, C. Y. C., Tellkamp, F., Günschmann, C., Dieterich, C., … Wickström, S. A. (2016). Mechanical regulation of transcription controls

Polycomb-mediated gene silencing during lineage commitment. *Nature Cell Biology*, *18*(8), 864–875. https://doi.org/10.1038/ncb3387

48. Lin, Y., & Xu, S. (2010). *AFM analysis of the lacunar-canalicular network in demineralized compact bone. Journal of Microscopy, 241(3), 291–302.* doi:10.1111/j.1365-2818.2010.03431.x

49. Gulhati, P., Bowen, K. A., Liu, J., Stevens, P. D., Rychahou, P. G., Chen, M., … Evers, B. M. (2011). mTORC1 and mTORC2 regulate EMT, motility, and metastasis of colorectal cancer via RhoA and Rac1 signaling pathways. *Cancer research, 71*(9), 3246–3256. doi:10.1158/0008-5472.CAN-10-4058

50. Isermann, P., & Lammerding, J. (2013). Nuclear mechanics and mechanotransduction in health and disease. *Current Biology*, *23*(24), R1113–R1121. https://doi.org/10.1016/j.cub.2013.11.0

51. Heo, S. J., Driscoll, T. P., Thorpe, S. D., Nerurkar, N. L., Baker, B. M., Yang, M. T., … Mauck, R. L. (2016). Differentiation alters stem cell nuclear architecture, mechanics, and mechano-sensitivity. *ELife*, *5*(2016), 1–21. https://doi.org/10.7554/eLife.18207

52. Bianco, P., Cao, X., Frenette, P. S., Mao, J. J., Robey, P. G., Simmons, P. J., & Wang, C. Y. (2013). The meaning, the sense and the significance: translating the science of mesenchymal stem cells into medicine. *Nature medicine*, *19*(1), 35–42. doi:10.1038/nm.3028

53. Armiento, A.R., Stoddart, M.J., Alini, M., Eglin, D., (2017) Biomaterials for Articular Cartilage Tissue Engineering: Learning from Biology., *Acta Biomaterialia*.

54. [234] Z. Li, L. Kupcsik, S.J. Yao, M. Alini, M.J. Stoddart, Mechanical load modulates chondrogenesis of human mesenchymal stem cells through the TGF-beta pathway, J Cell Mol Med 14(6A) (2010) 1338-46.

55. Kuo, Y. C., Chang, T. H., Hsu, W. T., Zhou, J., Lee, H. H., Hui-Chun Ho, J., … Kuang-Sheng, O. (2015). Oscillatory shear stress mediates directional reorganization of actin cytoskeleton and alters differentiation propensity of mesenchymal stem cells. *Stem Cells*, *33*(2), 429–442. https://doi.org/10.1002/stem.1860

56. Wang, X., Liu, H., Zhu, M., Cao, C., Xu, Z., Tsatskis, Y., … Sun, Y. (2018). Mechanical stability of the cell nucleus - roles played by the cytoskeleton in nuclear deformation and strain recovery. *Journal of Cell Science*, *131*(13). https://doi.org/10.1242/jcs.209627

57. Buxboim, A., Irianto, J., Swift, J., Athirasala, A., Shin, J. W., Rehfeldt, F., & Discher, D. E. (2017). Coordinated increase of nuclear tension and lamin-A with matrix stiffness outcompetes lamin-B receptor that favors soft tissue phenotypes. *Molecular Biology of the Cell*, *28*(23), 3333–3348. https://doi.org/10.1091/mbc.E17-06-0393

58. Nikolaev, N. I., Müller, T., Williams, D. J., & Liu, Y. (2014). Changes in the stiffness of human mesenchymal stem cells with the progress of cell death as measured by atomic force microscopy. *Journal of Biomechanics*, *47*(3), 625–630. https://doi.org/10.1016/j.jbiomech.2013.12.004

59. Dahl, K. N., Engler, A. J., Pajerowski, J. D., & Discher, D. E. (2005). Power-law rheology of isolated nuclei with deformation mapping of nuclear substructures. *Biophysical journal*, *89*(4), 2855–2864. doi:10.1529/biophysj.105.062554

60. Stephens, A. D., Banigan, E. J., Adam, S. A., Goldman, R. D., & Marko, J. F. (2017). Chromatin and lamin A determine two different mechanical response regimes of the cell nucleus. *Molecular Biology of the Cell*, *28*(14), 1984–1996. https://doi.org/10.1091/mbc.E16-09-0653

61. Sun, M., Chi, G., Xu, J., Tan, Y., Xu, J., Lv, S., … Li, Y. (2018). Extracellular matrix stiffness controls osteogenic differentiation of mesenchymal stem cells mediated

by integrin α5. *Stem cell research & therapy*, *9*(1), 52. doi:10.1186/s13287-018-0798-0

62. Mirjam Ketema, Arnoud Sonnenberg; Nesprin-3: a versatile connector between the nucleus and the cytoskeleton. *Biochem Soc Trans* 1 December 2011; 39 (6): 1719–1724.

63. Matsumoto, A., Hieda, M., Yokoyama, Y., Nishioka, Y., Yoshidome, K., Tsujimoto, M., & Matsuura, N. (2015). Global loss of a nuclear lamina component, lamin A/C, and LINC complex components SUN1, SUN2, and nesprin-2 in breast cancer. *Cancer medicine*, *4*(10), 1547–1557. doi:10.1002/cam4.495